AD 705 52

PROJECT THEMIS

DDC
DEC 15 1970
B

SCHOOL OF ENGINEERING
UNIVERSITY OF MASSACHUSETTS
AMHERST

IMPACT LOADING OF SUBMARINE HULLS

By

Frederick J. Dzialo

Contract No. ONR-N00014-68-A-0146-8
Report No. THEMIS-UM-70-2

DISTRIBUTION OF THIS DOCUMENT IS UNLIMITED

February 1970

Approved for Release

Reproduction in whole or in part is permitted for any purpose of the United States Government. This research was sponsored by the Office of Naval Research under ONR Contract No. N00014-68-A-0146, Subcontract No. N00014-68-A-0146-8, ONR Contract Authority Identification No. NR 200-016.

Charles E. Hutchinson
Co-Manager, Project THEMIS
University of Massachusetts

ABSTRACT

Following Flugge's exact derivation for the buckling of cylindrical shells, the equations of motion for dynamic loading of cylindrical shells subjected to hydrostatic and axial pressure have been formulated.

The equations of motion are applicable for long, short, or thick shells, and are very useful in calculating deflections and stresses when the impact loads are applied to comparatively small regions of the shell. The normal mode theory was utilized to provide dynamic solutions for the equations of motion.

Solutions are also provided for the Timoshenko-type theory, and comparisons are made between the two theories by considering and neglecting in-plane inertia forces.

Comparison of results is exemplified by a numerical example which considers the effect of hydrostatic pressure on the dynamic response of a shell simply supported by a thin diaphragm and subjected to a localized unit radial impulse.

ACKNOWLEDGEMENT

This research was accomplished with the support of the Office of Naval Research. Computations were done at the University of Massachusetts Research Computer Center, Amherst, Massachusetts. The author wishes to record his thanks to Messrs. Aarij and Minhaj Kirmani for their assistance in computer programming and calculations.

TABLE OF CONTENTS

		Page
ABSTRACT		iii
ACKNOWLEDGEMENT		iv
LIST OF TABLES		vii
LIST OF FIGURES		viii
I.	INTRODUCTION	1
	A. Applicability of Work	1
	B. Statement of Problem	1
II.	THEORY	2
	A. Equations of Motion	2
	B. Orthogonality and Modal Vibrations	4
	C. Solutions of Equations of Motion for Modal Vibration	6
III.	SOLUTIONS FOR FORCED VIBRATIONS	8
	A. Solution for Impact Loading	8
	B. Solution for Unit Impulse	9
IV.	SOLUTIONS FOR SYMMETRICAL VIBRATIONS	12
	A. Free Vibrations	13
	B. Forced Vibrations	14
V.	INTEGRAL OF THE SQUARE OF EIGENFUNCTIONS	14
VI.	ILLUSTRATIVE EXAMPLE FOR CYLINDER SUPPORTED BY THIN DIAPHRAGM	15
VII.	EQUATIONS OF MOTION FOR TIMOSHENKO THEORY	22
VIII.	DATA FOR ILLUSTRATIVE EXAMPLE FOR UNIT RADIAL IMPULSE	25

Page

IX. SUMMARY OF THEORETICAL RESULTS 26

A. Effect of Pressures on Natural Frequencies 26

B. Dynamic Response for Unit Radial Impulse 35

X. DISCUSSION AND CONCLUSIONS 46

XI. LITERATURE CITED 47

LIST OF TABLES

		Page
TABLE I	Effect of Hydrostatic Pressure on Frequencies in Buckling Mode, Flugge's Theory	26
TABLE II	Effect of Hydrostatic Pressure on Frequencies in Buckling Mode, Timoshenko's Theory	27
TABLE III	Effect of Hydrostatic Pressure on Frequencies in Buckling Mode, Flugge's Theory with and without Axial Inertia	28
TABLE IV	Effect of Hydrostatic Pressure on Frequencies in Buckling Mode, Timoshenko's Theory with and without Axial Inertia	29
TABLE V	Comparison of Frequencies for Various Mode Shapes, Flugge's Theory, n = 1, m = 1 - 10	30
TABLE VI	Comparison of Frequencies for Various Mode Shapes, Flugge's Theory, n = 3, m = 1 - 10	31
TABLE VII	Comparison of Frequencies for Various Mode Shapes, Flugge's Theory, n = 5, m = 1 - 10	32
TABLE VIII	Effect of Hydrostatic Pressure on Fundamental Frequency, Flugge's Theory	33
TABLE IX	Effect of Hydrostatic Pressure on Higher Frequencies, Flugge's Theory	34
TABLE X	Effect of Hydrostatic Pressure on Dynamic Response for Unit Impulse, Flugge's Theory	35
TABLE XI	Dynamic Response for Unit Impulse with and without In-Plane Inertia, Flugge's Theory	36
TABLE XII	Effect of Hydrostatic Pressure on Dynamic Response for Unit Impulse, Comparison of Theories with In-Plane Inertia Included	37
TABLE XIII	Dynamic Response for Unit Impulse with In-Plane Inertia, Comparison of Theories	38
TABLE XIV	Effect of Hydrostatic Pressure and Loading Area on Dynamic Response for Unit Impulse, Flugge's Theory with In-Plane Inertia Included	39

LIST OF FIGURES

		Page
FIGURE 1	Cylindrical Shell Subjected to Dynamic and Hydrostatic Loading	10
FIGURE 2	Radial Displacement versus Pressure for $\phi = 0$, $x = \ell/2$ at Various Values of Time	40
FIGURE 3	Radial Displacement versus Time for $P/P_c = 0$, $\phi = 0$, $x = \ell/2$ at Various Values of Time	41
FIGURE 4	Longitudinal Strain versus Time for $P/P_c = 0$, $\phi = 0$, $x = \ell/2$	42
FIGURE 5	Longitudinal Strain versus Time for $P/P_c = 0.5$, $\phi = 0$, $x = \ell/2$	43
FIGURE 6	Longitudinal Strain versus Time for $P/P_c = 0$, $\phi = 0$, $x = \ell/2$	44
FIGURE 7	Circumferential Strain versus Time for $P/P_c = 0$, $\phi = 0$, $x = \ell/2$	45

IMPACT LOADING OF SUBMARINE HULLS

Introduction

The purpose of this investigation is to determine the effect of impact loads on submarine hulls. For ductile materials current design methods utilize static loads for design with a performance criterion that the hull behave in a ductile manner when subjected to an impact load that may occur during ground collision or depth charges. Since glass, considered as a possible material for design has brittle properties the present design practices must be re-evaluated. Hence, more rigorous analyses must be made to determine the dynamic stress and deformation characteristics of glass hulls subjected to impact loads, and deep hydrostatic pressures. The present investigation will consider only the response of the shell. The coupled response of the shell and ring frames will be considered in a future investigation.

The model to be investigated will essentially be a cylindrical shell under deep hydrostatic and axial pressure, and subjected to an impact load.

Following Flugge's exact derivation for the buckling of cylindrical shells, the equations of motion are formulated. The equations are applicable for long, short or thick shells, and are very useful in calculating deflections and stresses when the impact loads are applied to comparatively small regions of the shell. The normal mode theory is utilized to provide dynamic solutions for the equations of motion.

Solutions are also provided for the Timoshenko-type theory, and comparisons are made between the two theories by considering and neglecting in-plane inertia forces.

Equations of Motion

Following Flugge's [1] exact derivation for the buckling of cylindrical shells, the differential equations of motion for impact loading of cylindrical shells under hydrostatic pressure become:

$$aN'_x + aN'_{\varphi x} - pa(u'' - w') - Pu'' + a^2 p_x = \rho h a^2 \frac{\partial^2 u}{\partial t^2} \tag{1}$$

$$aN'_\varphi + aN'_{x\varphi} - aQ_\varphi - pa(v'' + w') - Pv'' + a^2 p_\varphi = \rho h a^2 \frac{\partial^2 v}{\partial t^2} \tag{2}$$

$$-aQ'_\varphi - aQ'_x - aN_\varphi - pa(u' - v' + w'') - Pw'' + a^2 p_r$$

$$= \rho h a^2 \frac{\partial^2 w}{\partial t^2} \tag{3}$$

where

$$Q_\varphi = \frac{M'_\varphi + M'_{x\varphi}}{a} \tag{4}$$

$$Q_x = \frac{M'_x + M'_{\varphi x}}{a} \tag{5}$$

$$M_\varphi = \frac{D}{a}(v' + w + \nu u') + \frac{K}{a^2}(w + w'') \tag{6}$$

$$M_x = \frac{D}{a}(u' + \nu v' + \nu w) - \frac{K}{a^2} w'' \tag{7}$$

$$M_{\varphi x} = \frac{D}{a}\frac{1-\nu}{2}(u' + v') + \frac{K}{a^2}\frac{1-\nu}{2}(u' + w'') \tag{8}$$

$$H_{x\phi} = \frac{D}{a}\frac{1-\nu}{2}(u^{\cdot} + v') + \frac{K}{a^3}\frac{1-\nu}{2}(v' - w'^{\cdot}) \tag{9}$$

$$H_{\phi} = \frac{K}{a^2}(w + w^{\cdot\cdot} + \nu w'') \tag{10}$$

$$H_{x} = \frac{K}{a^2}(w'' + \nu w^{\cdot\cdot} - u' - \nu v^{\cdot}) \tag{11}$$

$$H_{\phi x} = \frac{K}{a^2}(1-\nu)(w'^{\cdot} + \frac{1}{2}u^{\cdot} - \frac{1}{2}v') \tag{12}$$

$$H_{x\phi} = \frac{K}{a^2}(1-\nu)(w'^{\cdot} - v') \tag{13}$$

Substitution of equations (4) through (13) into equations (1) through (3) yields:

$$u'' + \frac{(1-\nu)}{2}u^{\cdot\cdot} + \frac{1+\nu}{2}v'^{\cdot} + \nu w' + k\left(\frac{1-\nu}{2}u^{\cdot\cdot} - w''' + \frac{1-\nu}{2}w'^{\cdot\cdot}\right)$$
$$- q_1(u^{\cdot\cdot} - w') - q_2 u'' + \frac{p_x(x,t)a^2}{D} = \frac{\rho h a^2}{D}\frac{\partial^2 u}{\partial t^2} \tag{14}$$

$$\frac{1+\nu}{2}u'^{\cdot} + v^{\cdot\cdot} + \frac{1-\nu}{2}v'' + w^{\cdot} + k\left(\frac{3}{2}(1-\nu)v'' - \frac{3-\nu}{2}w''^{\cdot}\right)$$
$$- q_1(v^{\cdot\cdot} + w^{\cdot}) - q_2 v'' + \frac{p_\phi(x,t)a^2}{D} = \frac{\rho h a^2}{D}\frac{\partial^2 v}{\partial t^2} \tag{15}$$

$$\nu u' + v^{\cdot} + w + k\left(\frac{1-\nu}{2}u'^{\cdot\cdot} - u''' - \frac{3-\nu}{2}v''^{\cdot} + w''''\right.$$
$$\left. + 2w''^{\cdot\cdot} + w^{\cdot\cdot\cdot\cdot} + 2w^{\cdot\cdot} + w\right) + q_1(u' - v^{\cdot} + w^{\cdot\cdot})$$
$$+ q_2 w'' - \frac{p_r(x,t)a^2}{D} = \frac{-\rho h a^2}{D}\frac{\partial^2 w}{\partial t^2} \tag{16}$$

where

$$k = \frac{h^2}{12a^2}$$

$$q_1 = \frac{pa}{D}$$

$$q_2 = \frac{P}{D}$$

Equations (14) through (16) may be written:

$$\alpha_5 u'' + \alpha_2 u^{\cdot\cdot} + \frac{1+\nu}{2} v'^{\cdot} + \alpha_3 w' + k\left(\frac{1-\nu}{2} w'^{\cdot\cdot} - w'''\right) + \frac{p_x(x,t)}{D} a^2 = \frac{\rho h a^2}{D} \frac{\partial^2 u}{\partial t^2} \tag{17}$$

$$\frac{1+\nu}{2} u'^{\cdot} + \alpha_4 (v^{\cdot\cdot} + w^{\cdot}) + \alpha_1 v'' - \frac{k}{2}(3-\nu) w''^{\cdot} + \frac{p_\phi(x,t) a^2}{D} = \frac{\rho h a^2}{D} \frac{\partial^2 v}{\partial t^2} \tag{18}$$

$$\alpha_3 u' + \alpha_4 v^{\cdot} + (2k + 1 - \alpha_4) w^{\cdot\cdot} + k\left\{\frac{1-\nu}{2} u'^{\cdot\cdot} - u''' - \frac{3-\nu}{2} v''^{\cdot} + w'''' + 2w''^{\cdot\cdot} + w^{\cdot\cdot\cdot\cdot} + \left(\frac{k+1}{k}\right) w\right\} + (1 - \alpha_5) w'' - \frac{p_r(x,t) a^2}{D} = \frac{-\rho h a^2}{D} \frac{\partial^2 w}{\partial t^2} \tag{19}$$

where

$$\alpha_1 = \frac{1-\nu}{2}(1 + 3k) - q_2$$

$$\alpha_2 = \frac{1-\nu}{2}(1 + k) - q_1$$

$$\alpha_3 = (\nu + q_1)$$

$$\alpha_4 = 1 - q_1$$

$$\alpha_5 = 1 - q_2$$

Orthogonality and Modal Vibrations

For free vibrations, equations (1) through (3) become

$$aN'_x + aN^{\cdot}_{\phi x} - pa(u^{\cdot\cdot} - w') - Pu'' = \rho h a^2 \frac{\partial^2 u}{\partial t^2} \tag{20}$$

$$aN^{\cdot}_{\phi} + aN'_{x\phi} - aQ_{\phi} - pa(v^{\cdot\cdot} + w^{\cdot}) - Pv'' = \rho h a^2 \frac{\partial^2 v}{\partial t^2} \tag{21}$$

$$-aQ_{\phi}' - aQ_x' - aH_{\phi} - pa(u' - v' + w'') - Pw'' = \rho ha^2 \frac{\partial^2 w}{\partial t^2} \tag{22}$$

Equations (20) through (22) yield the free vibration frequencies and mode shapes. The orthogonality condition is derived by assuming that the displacements u, v, and w have the form

$$u = u_n(x, \phi)\, e^{i\omega_n t}, \qquad v = v_n(x, \phi)\, e^{i\omega_n t},$$
$$w = w_n(x, \phi) e^{i\omega_n t} \tag{23}$$

Finding the orthogonality condition involves the following steps: (1) the nth terms of expressions (23) are inserted into equations (20) through (22), and the resulting equations are multiplied by $u_m(x)$, $v_m(x)$ and $w_m(x)$, respectively, integrated over the domain, and added; (2) the mth terms of expressions (23) are inserted into equations (20) through (22), and the resulting equations are multiplied by $u_n(x)$, $v_n(x)$, and $w_n(x)$, respectively, integrated over the domain, and added; (3) the two equations resulting from Step 2 are subtracted from those resulting from Step 1; they are integrated by parts, and use is made of equations (4) through (13) to obtain the final orthogonality relation. The orthogonality condition may be written as follows:

$$\begin{aligned}
(\omega_n^2 - \omega_m^2) \int_0^L \rho h(u_n u_m + v_n v_m + w_n w_m)\, dx = \\
& u_n(H_{xm} + pw_m - P \frac{\partial u_m}{\partial x}) + v_n(H_{x\phi m} - \frac{M_{x\phi m}}{a} - P \frac{\partial v_m}{\partial x}) \\
& - w_n(Q_{xm} + P \frac{\partial w_m}{\partial x}) + M_{xm} \frac{\partial w_n}{\partial x} \\
& - u_m(H_{xn} + pw_n - P \frac{\partial u_n}{\partial x}) - v_m(N_{x\phi n} - \frac{M_{x\phi n}}{a} - P \frac{\partial v_n}{\partial x}) \\
& + w_m(Q_{xn} + P \frac{\partial w_n}{\partial x}) - M_{xn} \frac{\partial w_m}{\partial x} \Big\}_0^{\ell} = 0, \quad m \neq n
\end{aligned} \tag{24}$$

where the natural boundary conditions for the fixed, simply supported and free condition are given as:

Fixed at $x = 0, \ell$

$$u = v = w = \frac{\partial w}{\partial x} = 0 \tag{25}$$

Hinge at $x = 0, \ell$

$$u = v = w = 0$$

$$M_x = 0 \tag{26}$$

Simply Supported

at $x = 0, \ell$

$$w = 0$$

$$M_x = 0$$

$$N_{x\phi} - \frac{M_{x\phi}}{a} - P\frac{\partial v}{\partial x} = 0$$

$$N_x + pw - P\frac{\partial u}{\partial x} = 0 \tag{27}$$

Free at $x = 0, \ell$

$$M_x = 0$$

$$Q_x + P\frac{\partial w}{\partial x} = 0$$

$$N_{x\phi} - \frac{M_{x\phi}}{a} - P\frac{\partial v}{\partial x} = 0$$

$$N_x + pw - P\frac{\partial u}{\partial x} = 0 \tag{28}$$

The differential equations (17) - (19) may be solved by assuming

$$u = Ae^{\lambda x/a}\cos(m\phi)\, e^{i\omega t}$$

$$v = Be^{\lambda x/a}\sin(m\phi)\, e^{i\omega t} \tag{29}$$

$$w = Ce^{\lambda x/a}\cos(m\phi)\, e^{i\omega t}$$

Inserting equation (29) into equations (17) - (19) yields equation (30).

$$\begin{vmatrix} \alpha_5\lambda^2-m^2\alpha_2+(\rho ha^2\omega^2 mm/D) & (\frac{1+\nu}{2})m\lambda & \alpha_3\lambda-k(\frac{1-\nu}{2})m^2\lambda-k\lambda^3 \\ -(\frac{1+\nu}{2})m\lambda & -\alpha_4 m^2+\alpha_1\lambda^2+(\rho ha^2\omega^2 mm/D) & -\alpha_4 m+k(\frac{3-\nu}{2})m\lambda^2 \\ \alpha_3\lambda-k(\frac{1-\nu}{2})m^2\lambda-k\lambda^3 & \alpha_4 m-k(\frac{3-\nu}{2})m\lambda^2 & \begin{array}{l}-(2k+1-\alpha_4)m^2+1 \\ +(1-\alpha_5)\lambda^2 \\ +k[(\lambda^2-m^2)^2+1] \\ -\rho ha^2\omega^2_{mm}/D\end{array} \end{vmatrix} \begin{vmatrix} A \\ B \\ C \end{vmatrix} = 0 \tag{30}$$

The characteristic equation is found by setting the determinant of equation (30) equal to zero. To determine the eigenvalues, ω^2, the following method is utilized: A value of ω^2 is guessed and inserted into the characteristic equation. The characteristic equation will yield eight roots. For unequal roots, equations (29) may be written as follows:

$$u = \sum_{i=1}^{8} A_i e^{\lambda_i x/a}(\cos m\phi e^{i\omega t}), \quad v = \sum_{i=1}^{8} B_i e^{\lambda_i x/a}(\sin m\phi e^{i\omega t})$$
$$w = \sum_{i=1}^{8} C_i e^{\lambda_i x/a}(\cos m\phi)\, e^{i\omega t} \tag{31}$$

where for each λ_i there exists a relationship between the amplitudes A_i, B_i and C_i from the determinant of equation (30).

Equations (31) with the necessary boundary conditions will lead to a determinant $|a_{ij}|$. A plot is then made of the determinant $|a_{ij}|$ versus ω^2. The eigenvalues, ω^2, are those for which $|a_{ij}| = 0$. At a point, ω^2, when $|a_{ij}| = 0$, the ratio of the amplitudes A_i, B_i and C_i can be calculated from the determinant of equation (30).

For impact loads, local bending action will predominate, and the principal mode of response will be in the radial direction. Neglecting inertia forces in the longitudinal and circumferential directions, equation (30) reduces to equation (32).

$$\begin{vmatrix} \alpha_5 n^2 - m^2 \alpha_2 & \left(\frac{1+\nu}{2}\right) m n & \alpha_3 n - k\left(\frac{1-\nu}{2}\right) m^2 n - k n^3 \\ -\left(\frac{1+\nu}{2}\right) m n & -\alpha_4 m^2 + \alpha_1 n^2 & -\alpha_4 m + k\left(\frac{3-\nu}{2}\right) m n^2 \\ \alpha_3 n - k\left(\frac{1-\nu}{2}\right) m^2 n - k n^3 & -\alpha_4 m - k\left(\frac{3-\nu}{2}\right) m n^2 & \begin{array}{l} -(2k+1-\alpha_4) m^2 + 1 \\ +(1-\alpha_5) n^2 \\ +k[(n^2-m^2)^2+1] \\ +\rho h a^2 \omega_{nm}^2 / D \end{array} \end{vmatrix} \begin{vmatrix} A \\ B \\ C \end{vmatrix} = 0 \qquad (32)$$

Solutions for Forced Vibrations

Equations (17) through (19) may be solved by assuming

$$\begin{aligned} u &= \sum_{n=0}^{\infty} u_n(x, \phi)\, q_n(t) \\ v &= \sum_{n=0}^{\infty} v_n(x, \phi)\, q_n(t) \\ w &= \sum_{n=0}^{\infty} w_n(x, \phi)\, q_n(t) \end{aligned} \qquad (33)$$

Substituting the above equations into equations (17) through (19), and utilizing the orthogonality condition (24) yields the following:

$$q_n(t) = \frac{\int_0^{2\pi} \int_0^{\ell} \int_0^{t} [P_x(x,\phi,\lambda) u_n + P_\phi(x,\phi,\lambda) v_n + P_r(x,\phi,\lambda) w_n][\sin \omega_n (t-\lambda) d\lambda]\, dx\, d\phi}{\omega_n \int_0^{2\pi} \int_0^{\ell} \rho h (u_n^2 + v_n^2 + w_n^2)\, dx\, d\phi} \qquad (34)$$

For an impact loading as shown in Figure 1, equation (34) becomes

$$q_n(t) = \frac{\int_{(x-\varepsilon_1)/a}^{(x+\varepsilon_1)/a} \int_{\phi-\varepsilon_2}^{\phi+\varepsilon_2} \int_0^t [p_x(x,\phi,\lambda)u_n + p_\phi(x,\phi,\lambda)v_n + p_r(x,\phi,\lambda)w_n] \sin \omega_m(t-\lambda)\, d\lambda\, dx\, d\phi}{\omega_m \int_0^{2\pi} \int_0^{\ell} \rho h(u_n^2 + v_n^2 + w_n^2)\, dx\, d\phi} \tag{35}$$

For a concentrated impact loading, equation (34) becomes

$$q_n(t) = \frac{\lim_{\substack{\varepsilon_1 \to 0 \\ \varepsilon_2 \to 0}} \int_{(x-\varepsilon_1)/a}^{(x+\varepsilon_1)/a} \int_{\phi-\varepsilon_2}^{\phi+\varepsilon_2} \int_0^t [p_x(x, \phi, \lambda)u_n + p_\phi(x, \phi, \lambda)v_n + p_r(x, \phi, \lambda)w_n] \sin \omega_m(t - \lambda)\, d\lambda\, dx\, d\phi}{\omega_m \int_0^{2\pi} \int_0^{\ell} \rho h(u_n^2 + v_n^2 + w_n^2)\, dx\, d\phi} \tag{36}$$

where

$$p_x = \frac{P_x}{4\varepsilon_1\varepsilon_2}$$

$$p_\phi = \frac{P_\phi}{4\varepsilon_1\varepsilon_2}$$

$$p_r = \frac{P_r}{4\varepsilon_1\varepsilon_2}$$

Solution for Impulse

Consider an impulse per unit area, $i_x(x, \phi)$, $i_\phi(x, \phi)$ and $i_r(x, \phi)$ acting on the cylinder for an infinitely short time. The cylinder may now be considered to be vibrating freely with the following initial conditions:

At $t = 0$

$$u = v = w = 0 \tag{37}$$

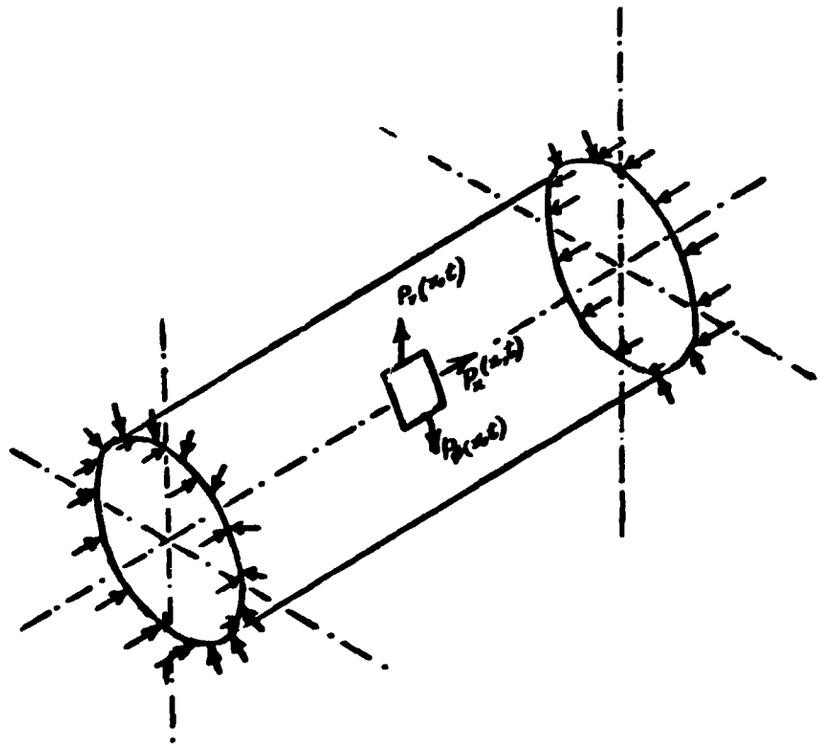

Figure 1-a

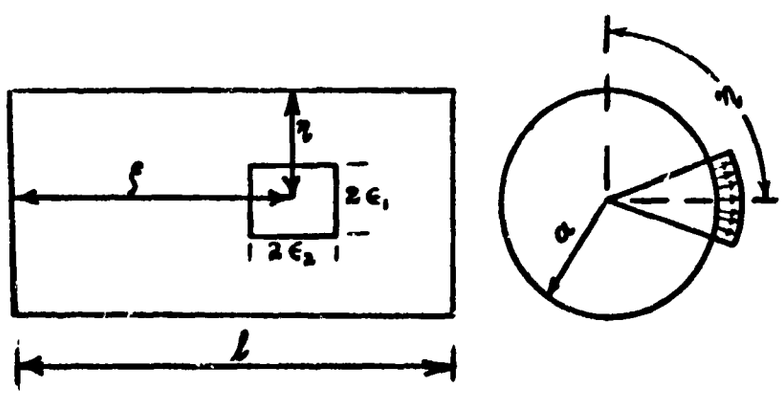

Figure 1-b

Cylindrical Shell Subjected to Dynamic and Hydrostatic Loading

At $t = 0$

$$\frac{\partial u}{\partial t} = \frac{i_x(x, \phi)}{\rho h}$$

$$\frac{\partial v}{\partial t} = \frac{i_\phi(x, \phi)}{\rho h} \tag{38}$$

$$\frac{\partial w}{\partial t} = \frac{i_r(x, \phi)}{\rho h}$$

The displacements for free vibrations are given as

$$u = \sum_{m=0}^{\infty} u_m(A_m \cos \omega_m t + B_m \sin \omega_m t)$$

$$v = \sum_{m=0}^{\infty} v_m(A_m \cos \omega_m t + B_m \sin \omega_m t) \tag{39}$$

$$w = \sum_{m=0}^{\infty} w_m(A_m \cos \omega_m t + B_m \sin \omega_m t)$$

Substituting the initial conditions (37) and (38) into equation (39) and making use of ortnogonality yields the following

$$u = \sum_{m=0}^{\infty} u_m B_m \sin \omega_m t$$

$$v = \sum_{m=0}^{\infty} v_m B_m \sin \omega_m t \tag{40}$$

$$w = \sum_{m=0}^{\infty} w_m B_m \sin \omega_m t$$

where

$$B_m = \frac{1}{\omega_m} \frac{\int_0^{2\pi} \int_0^{\ell} (i_x u_m + i_\phi v_m + i_r w_m)\, dx\, d\phi}{\int_0^{2\pi} \int_0^{\ell} \rho h(u_m^2 + v_m^2 + w_m^2)\, dx\, d\phi} \tag{41}$$

For a distributed impulse as shown in Figure 1, equation (41) becomes

$$B_m = \frac{\int_{(\eta-\varepsilon_1)/a}^{(\eta+\varepsilon_1)/a} \int_{\zeta-\varepsilon_2}^{\zeta+\varepsilon_2} [i_x u_m + i_\phi v_m + i_r w_m]\, dx\, d\phi}{\omega_m \int_0^{2\pi} \int_0^{\ell} \rho h(u_m^2 + v_m^2 + w_m^2)\, dx\, d\phi} \tag{42}$$

For a concentrated impulse, equation (41) becomes

$$B_m = \frac{\lim\limits_{\substack{\varepsilon_1 \to 0 \\ \varepsilon_2 \to 0}} \int_{(\eta-\varepsilon_1)/a}^{(\eta+\varepsilon_1)/a} \int_{\zeta-\varepsilon_2}^{\zeta+\varepsilon_2} [i_x u_m + i_\phi v_m + i_r w_m]\, dx\, d\phi}{\omega_m \int_0^{2\pi} \int_0^{\ell} \rho h(u_m^2 + v_m^2 + w_m^2)\, dx\, d\phi} \tag{43}$$

where

$$i_x = \frac{I_x}{4\varepsilon_1\varepsilon_2}$$

$$i_\phi = \frac{I_\phi}{4\varepsilon_1\varepsilon_2}$$

$$i_r = \frac{I_r}{4\varepsilon_1\varepsilon_2}$$

<u>Solutions for m = 0</u>

For n = 0, equations (1) through (3) and (14) through (16) degenerate to the following equations:

$$aN_x' + paw' - Pu'' + a^2 p_x = \rho h a^2 \frac{\partial^2 u}{\partial t^2} \tag{44}$$

$$aN_{x\phi}' - aQ_\phi - Pv'' + a^2 p_\phi = \rho h a^2 \frac{\partial^2 v}{\partial t^2} \tag{45}$$

$$-aQ_x' - aN_\phi - pau' - Pw'' + a^2 p_r = \rho h a^2 \frac{\partial^2 w}{\partial t^2} \tag{46}$$

$$\alpha_5 u'' + \alpha_3 w' - kw''' + (p_x a^2/D) = \frac{\rho h a^2}{D} \frac{\partial^2 u}{\partial t^2} \tag{47}$$

$$\alpha_1 v'' + (p_\phi a^2/D) = \frac{\rho h a^2}{D} \frac{\partial^2 v}{\partial t^2} \tag{48}$$

$$-\alpha_3 u' + k\{u''' - w'''' - (\frac{k+1}{k})w\} - (1 - \alpha_5)w''$$

$$+ (p_r a^2/D) = \frac{\rho h a^2}{D} \frac{\partial^2 w}{\partial t^2} \tag{49}$$

Solutions for equations (47) and (49) can be determined from the solutions given for unsymmetrical loading. For m = 0, equation (30) becomes

$$\begin{vmatrix} \alpha_5\lambda^2 + \frac{\rho h a^2 \omega_{no}^2}{D} & 0 & \alpha_3\lambda - k\lambda^3 \\ 0 & \alpha_1\lambda^2 + \frac{\rho h a^2 \omega_{no}^2}{D} & 0 \\ \alpha_3\lambda - k\lambda^3 & 0 & k\lambda^4 + (1 - \alpha_5)\lambda^2 + k + 1 - \frac{\rho h a^2}{D}\omega_{no}^2 \end{vmatrix} \begin{vmatrix} A \\ B \\ C \end{vmatrix} = 0 \qquad (50)$$

or

$$\lambda^6 + g_1\lambda^4 - g_2\lambda^2 - g_3 = 0 \qquad (51)$$

where

$$g_1 = [\alpha_5(1 - \alpha_5) + k(\frac{\rho h a^2 \omega^2}{D} + 2\alpha_3)]/k(\alpha_5 - k)$$

$$g_2 = [\alpha_3^2 - \alpha_5(1 + k) - (1 - 2\alpha_5)(\frac{\rho h a^2 \omega^2}{D})]/k(\alpha_5 - k)$$

$$g_3 = \frac{\rho h a^2 \omega^2}{D}(\frac{\rho h a^2 \omega^2}{D} - k - 1)/k(\alpha_5 - k)$$

Equations (47) through (49) are now uncoupled and may be solved independently.

The solution for equation (48) is as follows:

For free vibrations

$$v = A_1 \cos \sqrt{\rho h/D}\, \omega \frac{x}{a} + A_2 \sin \sqrt{\rho h/D}\, \omega \frac{x}{a} \qquad (52)$$

The orthogonality conditions are

$$(\omega_n^2 - \omega_m^2) \int_0^{\ell} \frac{\rho h a^2}{D} v_n v_m \, dx = \left| v_n \frac{\partial v_m}{\partial x} - v_m \frac{\partial v_n}{\partial x} \right|_0^{\ell}$$

The forced vibration solution becomes

$$v = \frac{\sum_{n=1}^{\infty} v_n \int_0^{\ell} \int_0^{t} p_r(x, \lambda)\, v_n \sin \omega_n(t - \lambda)\, d\lambda\, dx}{\omega_n \int_0^{\ell} \rho h v_n^2\, dx} \tag{53}$$

The orthogonality conditions from equation (24) become

$$\begin{aligned}
&(\omega_n^2 - \omega_m^2) \int_0^{\ell} \rho h(u_n u_m + w_n w_m)\, dx \\
&= [u_n(N_{xm} + p w_m - P \frac{\partial w_m}{\partial x}) - w_n(Q_{xm} + P \frac{\partial w_m}{\partial x}) \\
&\quad + M_{xm} \frac{\partial w_n}{\partial x} - u_m(N_{xn} + p w_n - P \frac{\partial w_n}{\partial x}) \\
&\quad + w_m(Q_{xn} + P \frac{\partial w_n}{\partial x}) - M_{xn} \frac{\partial w_m}{\partial x}\Big|_0^{\ell} = 0
\end{aligned} \tag{54}$$

The dynamic solutions from equations (33) and (34) are

$$\begin{aligned}
u &= \sum_{n=1}^{\infty} u_{on}(x)\, q_{on}(t) \\
w &= \sum_{n=1}^{\infty} w_{on}(x)\, q_{on}(t)
\end{aligned} \tag{55}$$

where

$$q_{on}(t) = \frac{\int_0^{\ell} [p_x(x, \lambda) u_{no} + p_r(x, \lambda) w_{no}] \sin \omega_{on}(t - \lambda)\, d\lambda\, dx}{\omega_{no} \int_0^{\ell} \rho h(u_{no}^2 + w_{no}^2)\, dx}$$

Integral of the Square of Eigenfunctions

The integral of the square of the eigenfunctions is evaluated from equation (24) by a limiting process. For any prescribed boundary condition, the evaluation of the integral may be determined as follows:

$$\int_0^{\ell} \rho h[u_n^2(x) + v_n^2(x) + w_n^2(x)]\, dx$$

$$= \lim_{\omega_m \to \omega_n} (-1/2\omega_m) \frac{d}{d\omega_m} \Big| u_n\left(N_{xm} + \rho w_m - P \frac{\partial u_m}{\partial x}\right)$$

$$+ v_n\left(N_{x\phi m} - \frac{M_{x\phi m}}{a} - P \frac{\partial v_m}{\partial x}\right) - w_n\left(Q_{xm} + P \frac{\partial w_m}{\partial x}\right) + M_{xm} \frac{\partial w_n}{\partial x}$$

$$- u_m\left(N_{xn} + \rho w_n - P \frac{\partial u_n}{\partial x}\right) - v_m\left(N_{x\phi n} - \frac{M_{x\phi n}}{a} - P \frac{\partial v_n}{\partial x}\right)$$

$$+ w_m\left(Q_{xn} + P \frac{\partial w_n}{\partial x}\right) - M_{xn} \frac{\partial w_m}{\partial x} \Big|_0^{\ell} \tag{56}$$

<u>Illustrative Example for Cylinder Supported by Thin Diaphragm</u>

For a cylinder supported by a thin diaphragm the following displacements satisfy the natural boundary conditions as derived from the orthogonality conditions:

$$u = \sum_m \sum_n U_{mn} \cos m\phi \cos \frac{n\pi x}{\ell}$$

$$v = \sum_m \sum_n V_{mn} \sin m\phi \sin \frac{n\pi x}{\ell} \tag{57}$$

$$w = \sum_m \sum_n W_{mn} \cos m\phi \sin \frac{n\pi x}{\ell}$$

To determine the natural frequencies and mode shapes the determinant for the frequency equation becomes

$$
\begin{bmatrix}
-\alpha_2\left(\frac{n\pi a}{\ell}\right)^2 - m^2\alpha_1 + \frac{\rho h a^2}{L}\,\Omega_{nm}^2 & \frac{1+\nu}{2}\, m\left(\frac{n\pi a}{\ell}\right) & \alpha_3\left(\frac{n\pi a}{\ell}\right) - k\left(\frac{1-\nu}{2}\right) m^2\left(\frac{n\pi a}{\ell}\right) + k\left(\frac{n\pi a}{\ell}\right)^3 & U_{mn} \\
\left(\frac{1+\nu}{2}\right) m\left(\frac{n\pi a}{\ell}\right) & -\alpha_4 m^2 - \alpha_1\left(\frac{n\pi a}{\ell}\right)^2 + \frac{\rho h a^2}{L}\,\Omega_{nm}^2 & -\alpha_4 m - k\left(\frac{3-\nu}{2}\right) m\left(\frac{n\pi a}{\ell}\right)^2 & V_{mn} \\
-\alpha_3\left(\frac{n\pi a}{\ell}\right) + \frac{k(1-\nu)}{2}\, m^2\left(\frac{n\pi a}{\ell}\right) - k\left(\frac{n\pi a}{\ell}\right)^3 & \alpha_4 m + k\left(\frac{3-\nu}{2}\right) m\left(\frac{n\pi a}{\ell}\right)^2 & -(2k+1-\alpha_4)m^2 + 1 - \left(\frac{n\pi a}{\ell}\right)^2(1-\alpha_5) + k\left[\left(\frac{n\pi a}{\ell}\right)^2 + m^2\alpha^2 + 1\right] - \frac{\rho h}{L}\, a^2\,\Omega_{mn}^2 & W_{mn}
\end{bmatrix} = 0
\tag{58}
$$

Solutions for Forced Vibrations

From equations (33) and (34) the dynamic displacements become

$$
\begin{aligned}
u &= \sum_m \sum_n U_{mn} \cos m\phi \left(\cos \frac{n\pi x}{\ell}\right) q_{mn}(t) \\
v &= \sum_m \sum_n V_{mn} \sin m\phi \left(\sin \frac{n\pi x}{\ell}\right) q_{mn}(t) \\
w &= \sum_m \sum_n W_{mn} \cos m\phi \left(\sin \frac{n\pi x}{\ell}\right) q_{mn}(t)
\end{aligned}
\tag{59}
$$

where

$$q_{mn}(t) = \int_0^{2\pi}\int_0^{\ell}\int_0^{t} [p_x(x, \phi, \lambda)U_{mn} \cos m\phi \cos \frac{n\pi x}{\ell}$$

$$+ p_\phi(x, \phi, \lambda)V_{mn} \sin m\phi \sin \frac{n\pi x}{\ell}$$

$$+ p_r(x, \phi, \lambda)W_{mn} \cos m\phi \sin \frac{n\pi x}{\ell}]$$

$$\times \left| \frac{\sin \omega_{mn}(t - \lambda)\, d\lambda\, dx\, d\phi}{\omega_{mn}\int_0^{2\pi}\int_0^{\ell} \rho h(U_{mn}^2 \cos^2 m\phi \cos^2 \frac{n\pi x}{\ell} + V_{mn}^2 \sin^2 m\phi \sin^2 \frac{n\pi x}{\ell} + W_{mn}^2 \cos^2 m\phi \sin^2 \frac{n\pi x}{\ell})\, dx\, d\phi} \right|$$

The ratio of the mode shape coefficients are

$$\alpha = \frac{U_{mn}}{W_{mn}} = \frac{-CD + BE}{AD - B^2}$$

$$\beta = \frac{V_{mn}}{W_{mn}} = \frac{-AE + BC}{AD - B^2} \tag{60}$$

where

$$A = -\alpha_5(\frac{n\pi a}{\ell})^2 - m^2\alpha_2 + \frac{\rho h a^2}{D}\omega_{mn}^2$$

$$B = \frac{1 + \nu}{2} m(\frac{n\pi a}{\ell})$$

$$C = \alpha_3(\frac{n\pi a}{\ell}) - k(\frac{1 - \nu}{2})m^2(\frac{n\pi a}{\ell}) + k(\frac{n\pi a}{\ell})^3$$

$$D = -\alpha_4 m^2 - \alpha_1(\frac{n\pi a}{\ell})^2 + \frac{\rho h a^2}{D}\omega_{mn}^2$$

$$E = -\alpha_4 m - k(\frac{3 - \nu}{2})m(\frac{n\pi a}{\ell})^2$$

For $m = 0$

$$q_{on}(t) = \int_0^{2\pi}\int_0^{\ell}\int_0^{t} [p_x(x, \phi, \lambda)U_{on} \cos \frac{n\pi x}{\ell} + p_r(x, \phi, \lambda)W_{on} \sin \frac{n\pi x}{\ell}]$$

$$\times \frac{\sin \omega_{on}(t - \lambda)\, d\lambda\, dx\, d\phi}{\omega_{on}\, \rho h \pi \ell (U_{on}^2 + W_{on}^2)} \tag{61}$$

For $m \neq 0$

$$q_{nm}(t) = \int_0^{2\pi} \int_0^{\ell} \int_0^{t} \Big[p_x(x, \phi, \lambda) U_{nm} \cos m\phi \cos \frac{n\pi x}{\ell}$$

$$+ p_\phi(x, \phi, \lambda) V_{nm} \sin m\phi \sin \frac{n\pi x}{\ell}$$

$$+ p_r(x, \phi, \lambda) W_{nm} \cos m\phi \sin \frac{n\pi x}{\ell} \Big]$$

$$\times \frac{\sin \omega_{nm}(t - \lambda)\, d\lambda\, dx\, d\phi}{\omega_{nm} \rho h \frac{\pi \ell}{2} (U_{nm}^2 + V_{nm}^2 + W_{nm}^2)} \tag{62}$$

<u>Solutions for Radial Impact</u>

a. Unit Step Loaded Distributed over Finite Area $(2\varepsilon_1 \cdot 2\varepsilon_2)$

$$u = \frac{4}{\rho h \pi^2} \left(\frac{\varepsilon_1}{a}\right) \sum_{n=1}^{\infty} \left(\frac{\alpha_{no}}{n}\right) \left(\frac{1}{\alpha_{no}^2 + 1}\right) \left(\sin \frac{n\pi\zeta}{\ell}\right) \left(\sin \frac{n\pi\varepsilon_2}{\ell}\right)$$

$$\times \left(\cos \frac{n\pi x}{\ell}\right) \left(\frac{1 - \cos \omega_{no} t}{\omega_{no}^2}\right)$$

$$+ \frac{8}{\rho h \pi^2} \sum_{n=1}^{\infty} \sum_{m=1}^{\infty} \left(\frac{\alpha_{nm}}{nm}\right) \left(\cos \frac{m\eta}{a}\right) \left(\sin \frac{n\pi\zeta}{\ell}\right) \left(\sin \frac{m\varepsilon_1}{a}\right) \left(\sin \frac{n\pi\varepsilon_2}{\ell}\right)$$

$$\times \cos m\phi \cos \frac{n\pi x}{\ell} \left(\frac{(1 - \cos \omega_{nm} t)}{\omega_{nm}^2 (\alpha_{nm}^2 + \beta_{nm}^2 + 1)}\right)$$

$$v = \frac{8}{\rho h \pi^2} \sum_{n=1}^{\infty} \sum_{m=1}^{\infty} \left(\frac{\beta_{nm}}{nm}\right) \left(\cos \frac{m\eta}{a}\right) \left(\sin \frac{n\pi\zeta}{\ell}\right) \left(\sin \frac{m\varepsilon_1}{a}\right) \left(\sin \frac{n\pi\varepsilon_2}{\ell}\right)$$

$$\times \sin m\phi \sin \frac{n\pi x}{\ell} \left(\frac{(1 - \cos \omega_{nm} t)}{\omega_{nm}^2 (\alpha_{nm}^2 + \beta_{nm}^2 + 1)}\right)$$

$$w = \frac{4}{\rho h \pi^2} \left(\frac{\varepsilon_1}{a}\right) \sum_{n=1}^{\infty} \left(\frac{1}{n}\right) \left(\sin \frac{n\pi\zeta}{\ell}\right) \sin \frac{n\pi\varepsilon_2}{\ell} \sin \frac{n\pi x}{\ell} \left(\frac{1 - \cos \omega_{no} t}{\omega_{no}^2 (\alpha_{no}^2 + 1)}\right)$$

$$+ \frac{8}{\rho h \pi^2} \sum_{n=1}^{\infty} \sum_{m=1}^{\infty} \left(\frac{1}{nm}\right) \left(\cos \frac{m\eta}{a}\right) \left(\sin \frac{n\pi\zeta}{\ell}\right) \left(\sin \frac{m\varepsilon_1}{a}\right) \left(\sin \frac{n\pi\varepsilon_2}{\ell}\right)$$

$$\times \cos m\phi \sin \frac{n\pi x}{\ell} \frac{(1 - \cos \omega_{nm} t)}{\omega_{nm}^2 (\alpha_{nm}^2 + \beta_{nm}^2 + 1)} \tag{63}$$

b. Concentrated Unit Step Load

$$u = \frac{1}{\pi\rho h a \ell} \sum_{n=1}^{\infty} \left(\frac{\alpha_{no}}{\alpha_{no}^2 + 1}\right)\left(\sin \frac{n\pi\zeta}{\ell}\right)\left(\cos \frac{n\pi x}{\ell}\right)\left(\frac{1 - \cos \omega_{no} t}{\omega_{no}^2}\right)$$

$$+ \frac{2}{\pi\rho h a \ell} \sum_{n=1}^{\infty} \sum_{m=1}^{\infty} \left(\frac{\alpha_{nm}}{\alpha_{nm}^2 + \beta_{nm}^2 + 1}\right)\left(\cos \frac{m\eta}{a}\right)\left(\sin \frac{n\pi\zeta}{\ell}\right)\left(\cos m\phi\right)$$

$$\times \left(\cos \frac{n\pi x}{\ell}\right)\left(\frac{1 - \cos \omega_{nm} t}{\omega_{nm}^2}\right)$$

$$v = \frac{2}{\pi\rho h a \ell} \sum_{n=1}^{\infty} \sum_{m=1}^{\infty} \left(\frac{\beta_{nm}}{\alpha_{nm}^2 + \beta_{nm}^2 + 1}\right)\left(\cos \frac{m\eta}{a}\right)\left(\sin \frac{n\pi\zeta}{\ell}\right)\left(\sin m\phi\right)$$

$$\times \left(\sin \frac{n\pi x}{\ell}\right)\left(\frac{1 - \cos \omega_{nm} t}{\omega_{nm}^2}\right) \tag{64}$$

$$w = \frac{1}{\pi\rho h a \ell} \sum_{n=1}^{\infty} \left(\frac{1}{\alpha_{no}^2 + 1}\right)\left(\sin \frac{n\pi\zeta}{\ell}\right)\left(\sin \frac{n\pi x}{\ell}\right)\left(\frac{1 - \cos \omega_{no} t}{\omega_{no}^2}\right)$$

$$+ \frac{2}{\pi\rho h a \ell} \sum \left(\frac{1}{\alpha_{nm}^2 + \beta_{nm}^2 + 1}\right)\left(\cos \frac{m\eta}{a}\right)\left(\sin \frac{n\pi\zeta}{\ell}\right)\left(\cos m\phi\right)$$

$$\times \left(\sin \frac{n\pi x}{\ell}\right)\left(\frac{1 - \cos \omega_{nm} t}{\omega_{nm}^2}\right)$$

c. Unit Impulse

Solutions for a unit impulse can be found by differentiating with respect to time the solutions for a unit step function. A typical displacement relationship for a concentrated unit impulse is as follows:

$$u = \frac{1}{\pi\rho h a \ell} \sum_{n=1}^{\infty} \left(\frac{\alpha_{no}}{\alpha_{no}^2 + 1}\right)\left(\sin \frac{n\pi\zeta}{\ell}\right)\left(\cos \frac{n\pi x}{\ell}\right)\left(\frac{\sin \omega_{no} t}{\omega_{no}}\right)$$

$$+ \frac{2}{\pi\rho h a \ell} \sum_{n=1}^{\infty} \sum_{m=1}^{\infty} \left(\frac{\alpha_{nm}}{\alpha_{nm}^2 + \beta_{nm}^2 + 1}\right)\left(\cos \frac{m\eta}{a}\right)\left(\sin \frac{n\pi\zeta}{\ell}\right)$$

$$\times \left(\cos m\phi\right)\left(\cos \frac{n\pi x}{\ell}\right)\left(\frac{\sin \omega_{nm} t}{\omega_{nm}}\right) \tag{65}$$

4. Triangular Loading with Suddenly Applied Value of Unity, and Decreasing Linearly to Zero at Time, t_d

$$u = \frac{4}{\rho h \pi^2}\left(\frac{\epsilon_1}{a}\right)\sum_{n=1}^{\infty}\left(\frac{\alpha_{no}}{n}\right)\left(\frac{1}{\alpha_{no}^2+1}\right)\left(\sin\frac{n\pi\zeta}{\ell}\right)\left(\sin\frac{n\pi\zeta_2}{\ell}\right)\left(\cos\frac{n\pi x}{\ell}\right)(F_{no}(t))$$

$$+\frac{8}{\rho h \pi^2}\sum_{n=1}^{\infty}\sum_{m=1}^{\infty}\left(\frac{\alpha_{nm}}{nm}\right)\left(\cos\frac{m\eta}{a}\right)\left(\sin\frac{n\pi\zeta}{\ell}\right)\left(\sin\frac{m\epsilon_1}{a}\right)\left(\sin\frac{n\pi\zeta_2}{\ell}\right)$$

$$\times(\cos m\phi)\left(\cos\frac{n\pi x}{\ell}\right)\frac{(F_{nm}(t))}{(\alpha_{nm}^2+\beta_{nm}^2+1)}$$

$$v = \frac{8}{\rho h \pi^2}\sum_{n=1}^{\infty}\sum_{m=1}^{\infty}\left(\frac{\beta_{nm}}{nm}\right)\left(\cos\frac{m\eta}{a}\right)\left(\sin\frac{n\pi\zeta}{\ell}\right)\left(\sin\frac{m\epsilon_1}{a}\right)\left(\sin\frac{n\pi\zeta_2}{\ell}\right)$$

$$\times(\sin m\phi)\left(\sin\frac{n\pi x}{\ell}\right)\frac{(F_{nm}(t))}{(\alpha_{nm}^2+\beta_{nm}^2+1)} \tag{56}$$

$$w = \frac{4}{\rho h \pi^2}\left(\frac{\epsilon_1}{a}\right)\sum_{n=1}^{\infty}\left(\frac{1}{n}\right)\left(\frac{1}{\alpha_{no}^2+1}\right)\left(\sin\frac{n\pi\zeta}{\ell}\right)\left(\sin\frac{n\pi\zeta_2}{\ell}\right)\left(\sin\frac{n\pi x}{\ell}\right)(F_o(t))$$

$$+\frac{8}{\rho h \pi^2}\sum_{n=1}^{\infty}\sum_{m=1}^{\infty}\left(\frac{1}{nm}\right)\left(\cos\frac{m\eta}{a}\right)\left(\sin\frac{n\pi\zeta}{\ell}\right)\left(\sin\frac{m\epsilon_1}{a}\right)\left(\sin\frac{n\pi\zeta_2}{\ell}\right)$$

$$(\cos m\phi)\left(\sin\frac{n\pi x}{\ell}\right)\frac{(F_{nm}(t))}{(\alpha_{nm}^2+\beta_{nm}^2+1)}$$

where

$$F_{no}(t) = \frac{1}{\omega_{no}^2}\left(1 - \cos\omega_{no}t + \frac{\sin\omega_{no}t}{\omega_{no}t_d} - \frac{t}{t_d}\right)$$

$$F_{nm}(t) = \frac{1}{\omega_{nm}^2}\left(1 - \cos\omega_{nm}t + \frac{\sin\omega_{nm}t}{\omega_{nm}t_d} - \frac{t}{t_d}\right) \qquad t \le t_d$$

$$F_{no}(t) = \frac{1}{\omega_{no}^3 t_d}\left(\sin\omega_{no}t - \sin\omega_{no}(t - t_d) - \frac{1}{\omega_{no}^2}\cos\omega_{no}t\right)$$

$$F_{nm}(t) = \frac{1}{\omega_{nm}^3 t_d}(\sin\omega_{nm}t - \sin\omega_{nm}(t - t_d)) - \frac{1}{\omega_{nm}^2}\cos\omega_{nm}t$$

$$t \ge t_d$$

e. Rectangular Pulse Loading with Suddenly Applied Value of Unity and Duration, t_d

Expressions for u, v, and w are identical to those corresponding to a triangular loading with the exception that $F_{no}(t)$ and $F_{nm}(t)$ be defined as follows:

$$
\begin{aligned}
F_{no}(t) &= \frac{1}{\omega_{no}^2}(1 - \cos \omega_{no} t) \\
F_{nm}(t) &= \frac{1}{\omega_{nm}^2}(1 - \cos \omega_{nm} t) \qquad t \leq t_d \\
F_{no}(t) &= \frac{1}{\omega_{no}^2}\left\{\cos \omega_{no}(t - t_d) - \cos \omega_{no} t\right\} \\
F_{nm}(t) &= \frac{1}{\omega_{nm}^2}\left\{\cos \omega_{nm}(t - t_d) - \cos \omega_{nm} t\right\} \qquad t \geq t_d
\end{aligned}
\tag{67}
$$

Equations of Motion for Timoshenko Theory

Equations (1) through (3) can be reduced to those presented by Timoshenko and Gere by assuming the following conditions:

a. The circumferential strain ε_ϕ, ε_x and $\gamma_{x\phi}$ are equal to zero in calculation of X_ϕ and $X_{x\phi}$.

b. Membrane forces are not affected by bending stresses, nor bending moments by membrane stresses.

Assumptions (a) and (b) yield $N_{\phi x} = N_{x\phi}$ and $M_{\phi x} = M_{x\phi}$. Assuming $\varepsilon_\phi = (v^{\cdot} + w)/a$; u', $u'' = 0$, and $\gamma_{x\phi} = (u^{\cdot} + v')/a = 0$, equations (1) through (3) become:

$$aN'_x + aN^{\cdot}_{\phi x} + pa(v'^{\cdot} + w') + a^2 p_x = \rho h a^2 \frac{\partial^2 u}{\partial t^2} \tag{68}$$

$$aN^{\cdot}_\phi + aN'_{x\phi} - aQ_\phi - Pv'' + a^2 p_\phi = \rho h a^2 \frac{\partial^2 v}{\partial t^2} \tag{69}$$

$$-aQ^{\cdot}_\phi - aQ'_x + aN_\phi - pa(w^{\cdot\cdot} + w) - Pw'' - a^2 p_r = \rho h a^2 \frac{\partial^2 w}{\partial t^2} \tag{70}$$

The membrane forces and moments from equations (6) through (13) become

$$N_\phi = \frac{D}{a}(v^{\cdot} + w + \nu u')$$

$$N_x = \frac{D}{a}(u' + \nu v^{\cdot} + \nu w)$$

$$N_{\phi x} = \frac{D}{a}\left(\frac{1-\nu}{2}\right)(u^{\cdot} + v')$$

$$N_{x\phi} = \frac{D}{a}\left(\frac{1-\nu}{2}\right)(u^{\cdot} + v')$$

$$M_\phi = \frac{K}{a^2}(-v^{\cdot} + w^{\cdot\cdot} + \nu w'')$$

$$M_x = \frac{K}{a^2}(w'' + \nu w^{\cdot\cdot} - \nu v^{\cdot})$$

$$M_{\phi x} = \frac{K}{a^2}(1 - \nu)(w'' - v')$$

$$M_{x\phi} = \frac{K}{a^2}(1 - \nu)(w'' - v') \tag{71}$$

Substitution of equations (71) into equations (68) - (70) yields the following:

$$u'' + \left(\frac{1 + \nu}{2}\right)v'' + \frac{1 - \nu}{2}u'' + \nu w' + q_1(v'' + w')$$
$$+ \frac{a^2 p_x}{D} = \frac{\rho h a^2}{D}\frac{\partial^2 u}{\partial t^2} \tag{72}$$

$$\left(\frac{1 + \nu}{2}\right)u'' + v'' + \left(\frac{1 - \nu}{2}\right)v'' + w' - k[w''' + w''']$$
$$+ k[(1 - \nu)v'' + v''] - q_2 v'' + \frac{a^2 p_\phi}{D} = \frac{\rho h a^2}{D}\frac{\partial^2 v}{\partial t^2} \tag{73}$$

$$\nu u' + v' + w + k[w'''' + 2w''' + w''''] - k[v''' + (2 - \nu)v''']$$
$$+ q_2 w'' + q_1(w'' + w) - \frac{a^2 p_r}{D} = \frac{-\rho h a^2}{D}\frac{\partial^2 w}{\partial t^2} \tag{74}$$

Equations (72) - (74) may be written

$$u'' + \frac{1 - \nu}{2}u'' + \beta_1 v'' + \beta_2 w' + a^2\frac{p_x}{D} = \frac{\rho h a^2}{D}\frac{\partial^2 u}{\partial t^2} \tag{75}$$

$$\left(\frac{1 + \nu}{2}\right)u'' + \beta_3 v'' + \beta_4 v'' + w' - k(w''' + w''')$$
$$+ \frac{a^2 p_\phi}{D} = \frac{\rho h a^2}{D}\frac{\partial^2 v}{\partial t^2} \tag{76}$$

$$\nu u' + v' + \beta_5 w + k(w'''' + 2w''' + w'''') - k[v''' + (2 - \nu)v''']$$
$$+ q_2 w'' + q_1 w'' - \frac{a^2 p_r}{D} = \frac{-\rho h a^2}{D}\frac{\partial^2 w}{\partial t^2} \tag{77}$$

where

$$\frac{1 + \nu}{2} + q_1 = \beta_1$$

$$\nu + q_1 = \beta_2$$

$$k + 1 = \beta_3$$

$$(1 - \nu)(k + \tfrac{1}{2}) - q_2 = \beta_4$$

$$1 + q_1 = \beta_5$$

$$\begin{bmatrix} -(\frac{n\pi a}{\ell})^2 - (\frac{1-\nu}{2})m^2 + \frac{\rho h a^2}{D}\omega_{mn}^2 & \beta_1(\frac{n\pi a}{\ell})m & \beta_2(\frac{n\pi a}{\ell}) \\ (\frac{1+\nu}{2})(\frac{n\pi a}{\ell})m & -\beta_3 m^2 - \beta_4(\frac{n\pi a}{\ell})^2 + \frac{\rho h a^2}{D}\omega_{mn}^2 & -m - k[(\frac{n\pi a}{\ell})^2 m + m^3] \\ -\nu(\frac{n\pi a}{\ell}) & m + k[+m^3 + (2-\nu)(\frac{n\pi a}{\ell})^2 m] & k[(\frac{n\pi a}{\ell})^2 + m^2]^2 + \beta_5 - q_2(\frac{n\pi a}{\ell})^2 - q_1 m^2 - \frac{\rho h a^2}{D}\omega_{mn}^2 \end{bmatrix} \begin{bmatrix} U_{mn} \\ V_{mn} \\ W_{mn} \end{bmatrix} \qquad (78)$$

Data for Illustrative Example for Unit Radial Impulse

h = 1.2 inches a = 60 inches ℓ = 24 inches

ℓ_1 = 12 inches ℓ_1 = 2 inches ℓ_2 = 2 inches

θ = 0 radians ν = 0.33333 n = 1 - 30 m = 0 - 29

$P_{c(Flugge)}$ = 5083.855 psi $P_{c(Timoshenko)}$ = 5071.773 psi

TABLE 1

EFFECT OF HYDROSTATIC PRESSURE ON FREQUENCIES IN BUCKLING MODE

Material: Steel

Parameters: $h/2a = 0.01$ $t/2a = 0.2$

Buckling Mode: $n = 1$, $m = 9$

Buckling Pressure: $P_c = 5083.755$

Flugge's Theory

	Including Axial Inertia			Neglecting Axial Inertia
P/P_c	f_1	f_2	f_3	f_1
0	517.04	3936.33	6807.24	519.73
0.2	462.47	3929.76	6803.23	464.91
0.4	400.52	3922.72	6799.21	402.62
0.6	327.93	3915.64	6795.19	328.74
0.8	231.25	3906.55	6791.18	232.46
1.0	---	---	---	---

TABLE II

EFFECT OF HYDROSTATIC PRESSURE ON FREQUENCIES IN BUCKLING MODE

Material: steel

Parameters: $h/2a = 0.01$ $\ell/2a = 0.2$

Buckling Mode: $n = 1$, $m = 9$

Buckling Pressure: 5071.793

Timoshenko's Theory

	Including Axial Inertia			Neglecting Axial Inertia
P/P_c	f_1	f_2	f_3	f_1
0	517.05	3937.01	6807.29	519.82
0.2	462.47	3933.98	6807.90	464.94
0.4	400.51	3930.95	6808.52	402.65
0.6	327.02	3927.92	6809.14	328.76
0.8	231.24	3924.90	6809.75	232.47
1.0	---	---	---	---

TABLE III

EFFECT OF HYDROSTATIC PRESSURE ON FREQUENCIES IN BUCKLING MODE

Material: steel

Parameters: $h/2a = 0.1$ $\ell/2a = 3$

Buckling Mode: $n = 1$, $m = 2$

Buckling Pressure, $P_c = 68811.45$

Flugge's Theory

	Including Axial Inertia			Neglecting Axial Inertia
P/P_c	f_1	f_2	f_3	f_1
0	889.93	6634.11	12765.31	997.21
0.2	796.08	6613.89	12750.83	891.93
0.4	689.51	6593.61	12736.34	772.44
0.6	563.06	6573.27	12721.83	630.69
0.8	398.19	6552.86	12707.32	445.97
1.0	---	---	---	---

TABLE IV

EFFECT OF HYDROSTATIC PRESSURE ON FREQUENCIES IN BUCKLING MODE

Material: Steel

Parameters: $h/2a = 0.1$ $\ell/2a = 8$

Buckling mode: $n = 1$, $m = 2$

Buckling Pressure, $P_c = 68356.4$

Timoshenko's Theory

	Including Axial Inertia			Neglecting Axial Inertia
P/P_c	f_1	f_2	f_3	f_1
0	886.62	6623.81	12811.59	995.52
0.2	793.12	6623.57	12810.07	890.42
0.4	686.95	6623.34	12808.54	771.13
0.6	560.96	6623.12	12807.03	629.63
0.8	396.71	6622.89	12805.51	445.21
1.0	---	---	---	---

TABLE V

COMPARISON OF FREQUENCIES FOR VARIOUS MODE SHAPES

Flugge's Theory

Parameters: $h/2a = 0.01$ $\ell/2a = 0.2$

$n = 1$

	$P/P_c = 0$			$P/P_c = 0.5$		
i	f_1	f_2	f_3	f_1	f_2	f_3
0	572.40	2579.58	4471.88	537.79	2572.29	4467.77
1	565.22	2601.76	4508.18	529.15	2594.27	4503.96
2	545.75	2666.71	4615.37	505.12	2658.64	4610.85
3	519.28	2770.30	4788.65	470.58	2761.32	4783.66
4	492.44	2907.31	5021.12	431.69	2897.20	5015.50
5	471.53	3072.65	5304.90	394.67	3061.23	5298.54
6	461.46	3261.81	5632.13	365.24	3248.95	5624.92
7	465.25	3470.96	5995.59	348.42	3456.57	5987.48
8	483.95	3696.87	6389.04	347.99	3680.88	6379.98
9	517.04	3936.83	6807.24	365.62	3919.18	6797.20
10	563.17	4188.57	7245.89	400.58	4169.22	7234.85

TABLE VI

COMPARISON OF FREQUENCIES FOR VARIOUS MODE SHAPES

Flugge's Theory

Parameters: $h/2a = 0.01$ $\ell/2a = 0.2$

$n = 3$

	$P/P_c = 0$			$P/P_c = 0.5$		
m	f_1	f_2	f_3	f_1	f_2	f_3
0	1899.26	7738.74	13404.75	1807.77	7716.36	13392.16
1	1902.11	7745.76	13416.82	1810.44	7723.81	13404.20
2	1910.69	7766.78	13452.99	1818.46	7744.65	13440.26
3	1925.04	7801.68	13513.04	1831.89	7779.25	13500.14
4	1945.25	7850.26	13596.67	1850.85	7827.42	13583.54
5	1971.41	7912.26	13703.44	1875.45	7888.90	13690.02
6	2003.66	7987.35	13832.83	1905.85	7963.35	13819.04
7	2042.11	8075.15	13984.19	1942.21	8050.42	13969.98
8	2086.89	8175.24	14156.82	1984.69	8149.68	14142.14
9	2138.13	8287.15	14349.96	2033.47	8260.67	14334.76
10	2195.92	8410.40	14562.79	2088.67	8382.92	14547.01

TABLE VII

COMPARISON OF FREQUENCIES FOR VARIOUS TABLE SHAPES

Flugge's Theory

Parameters: $h/2a = 0.01$ $\ell/2a = 0.2$

$n = 5$

	$P/P_c = 0$			$P/P_c = 0.5$		
m	f_1	f_2	f_3	f_1	f_2	f_3
0	5091.63	12897.91	22339.84	4993.41	12861.43	22318.32
1	5094.85	12902.10	22347.08	5001.56	12865.59	22326.04
2	5104.51	12914.67	22368.80	5011.04	12878.05	22347.70
3	5120.61	12935.60	22404.95	5026.84	12898.80	22383.75
4	5143.16	12964.84	22455.46	5048.97	12927.79	22434.12
5	5172.16	13002.34	22520.24	5077.44	12964.97	22498.72
6	5207.62	13048.02	22599.16	5112.25	13010.27	22577.42
7	5249.56	13101.79	22692.08	5153.44	13063.59	22670.07
8	5297.97	13163.56	22798.82	5200.99	13124.84	22776.52
9	5352.83	13233.21	22919.20	5254.96	13193.90	22896.56
10	5414.29	13310.62	23052.99	5315.34	13270.66	23029.97

TABLE VIII

EFFECT OF HYDROSTATIC PRESSURE ON FUNDAMENTAL FREQUENCY

Parameters: $h/2a = 0.01$ $\ell/2a = 0.2$ $P_c = 5083.855$

P/P_c	n, m	f
0	1, 6	461.46
0.2	1, 7	422.42
0.4	1, 7	374.72
0.6	1, 8	313.82
0.8	1, 8	230.72
0.95	1, 9	115.63
0.98	1, 9	73.13
1.00	1, 9	0.00

TABLE IX

EFFECT OF HYDROSTATIC PRESSURE ON HIGHER FREQUENCIES

Flugge's Theory

Parameters: $h/2a = 0.01$ $\ell/2a = 0.2$

$m = 10$

	$P/P_c = 0$			$P/P_c = 0.5$		
n	f_1	f_2	f_3	f_1	f_2	f_3
1	563.17	4188.57	7245.89	400.58	4169.22	7234.85
2	1196.55	6123.37	10597.00	1077.53	6100.93	10584.18
3	2195.92	8410.40	14562.79	2088.67	8382.92	14547.01
4	3600.27	10830.29	18756.15	3498.39	10796.81	18736.89
5	5414.29	13310.62	23052.99	5315.33	13270.66	23029.97

TABLE X

EFFECT OF HYDROSTATIC PRESSURE ON DYNAMIC RESPONSE FOR UNIT IMPULSE

Flugge's Theory

Time = 0.0006 sec P_c = 5071.793

		P/P_c	$u \times 10^{12}$	$v \times 10^{5}$	$w \times 10^{2}$	$\varepsilon_x \times 10^{5}$	$\varepsilon_\phi \times 10^{4}$	$\gamma_{x\phi} \times 10^{13}$	σ_x	σ_ϕ	$\tau_{x\phi} \times 10^{6}$
With In-Plane Inertia	$\phi = 0$	0	-2.7277	0.0000	2.9461	-3.3372	2.7508	0.0000	1968.3	8908.5	0.0000
		0.25	0.4485	0.0000	3.5206	-2.0180	2.8794	0.0000	2558.3	9449.1	0.0000
		0.50	4.3863	0.0000	4.2052	-0.2079	2.9856	0.0000	3288.7	10053.0	0.0000
		0.75	9.5507	0.0000	5.0308	2.140	3.0685	0.0000	4174.5	10597.0	0.0000
	$\phi = \pi/2$	0	0.5760	4.0157	-0.0656	-0.1681	-0.0582	-2.3409	-122.3	-215.5	-2.6336
		0.25	0.5523	4.2870	-0.0646	-0.2117	-0.0576	-2.3987	-136.2	-218.2	-2.6985
		0.50	0.5073	4.4458	-0.0589	-0.1895	-0.0569	-2.3412	-128.0	-213.5	-2.6338
		0.75	0.7580	4.4566	-0.0486	-0.1261	-0.0562	-2.1625	-105.8	-203.9	-2.4329
Without In-Plane Inertia	$\phi = 0$	0	-6.9778	0.0000	2.9403	-2.6418	2.8352	0.0000	2298.0	9271.6	0.0000
		0.25	-3.8182	0.0000	3.5164	-1.2752	2.9730	0.0000	2914.2	9890.4	0.0000
		0.50	0.299	0.0000	4.2035	0.5278	3.0853	0.0000	3649.1	10472.0	0.0000
		0.75	5.5291	0.0000	5.0327	0.2847	3.1696	0.0000	4527.0	11018.0	0.0000
	$\phi = \pi/2$	0	1.2938	1.0068	-0.0457	0.5808	-0.0562	-2.5181	189.7	46.37	-2.8329
		0.25	1.2645	1.2954	-0.0449	0.5879	-0.0457	-2.617	193.3	50.72	-2.9446
		0.50	1.2295	1.4828	-0.0398	0.5982	-0.0033	-2.566	198.2	56.22	-2.8862
		0.75	1.1860	1.5337	-0.0299	0.6123	-0.0018	-2.349	204.6	62.75	-2.6430

TABLE XI

DYNAMIC RESPONSE FOR UNIT IMPULSE WITH AND WITHOUT IN-PLANE INERTIA

Flugge's Theory

Time = 0.0006 sec $P/P_c = 0.5$

Including In-Plane Inertia

ϕ	$u \times 10^{12}$	$v \times 10^{5}$	$w \times 10^{2}$	$\varepsilon_x \times 10^{5}$	$\varepsilon_\phi \times 10^{4}$	$\gamma_{x\phi} \times 10^{12}$	σ_x	σ_ϕ	$\tau_{x\phi} \times 10^{5}$
0	4.3863	0.0000	4.2052	-0.2079	2.9856	0.0000	3288.70	10053.00	0.0000
$\pi/4$	-1.3593	-1.0792	0.2489	-0.5523	-0.0021	1.1629	-188.76	-69.21	1.3083
$\pi/2$	0.5073	4.4458	-0.0589	-0.1895	-0.0569	-0.2341	-128.00	-213.45	-0.2634
$3\pi/4$	0.3238	-1.5013	-0.0361	0.1045	-0.0392	0.1412	-8.82	-120.53	-0.1589
π	0.5995	0.0000	0.0180	0.2459	-0.0362	0.0000	42.27	-94.49	0.0000

Neglecting In-Plane Inertia

0	0.2987	0.0000	4.2035	0.5278	3.0853	0.0000	3649.10	10472.00	0.0000
$\pi/4$	2.7424	4.5379	0.2693	1.2245	-0.00451	0.5581	408.19	122.53	0.6279
$\pi/2$	1.2295	1.4828	-0.0398	0.5982	-0.00328	-0.2566	198.19	56.22	-0.2886
$3\pi/4$	1.3112	-1.2071	-0.01681	0.6377	-0.00178	0.1667	213.23	65.74	-0.1875
π	1.5129	0.0000	0.03737	0.7256	0.00408	0.0000	249.47	95.39	0.0000

TABLE XII

EFFECT OF HYDROSTATIC PRESSURE ON DYNAMIC RESPONSE FOR UNIT IMPULSE

Comparison of Theories with In-Plane Inertia Included

Time = 0.0006 sec

		P/P_c	$u \times 10^{12}$	$v \times 10^{5}$	$w \times 10^{2}$	$\varepsilon_x \times 10^{5}$	$\varepsilon_\phi \times 10^{4}$	$\gamma_{x\phi} \times 10^{13}$	σ_x	σ_ϕ	$\tau_{x\phi} \times 10^{6}$
Flugge's Theory	$\phi = 0$	0	-2.7277	0.0000	2.9461	-3.3372	2.7508	0.0000	1968.3	8908.5	0.0000
		0.25	0.4485	0.0000	3.5206	-2.0180	2.8794	0.0000	2558.3	9491.0	0.0000
		0.50	4.3863	0.0000	4.2052	-0.2079	2.9856	0.0000	3288.7	10053.0	0.0000
		0.75	9.5507	0.0000	5.0308	2.140	3.0685	0.0000	4174.5	10597.0	0.0000
	$\phi = \pi/2$	0	0.5760	4.0157	-0.0656	-0.1681	-0.0582	-2.3409	-122.3	-215.5	-2.6336
		0.25	0.5523	4.2870	-0.0646	-0.2117	-0.0576	-2.3987	-136.2	-218.2	-2.6985
		0.50	0.5073	4.4458	-0.0589	-0.1895	-0.0569	-2.3412	-128.0	-213.5	-2.6338
		0.75	0.7580	4.4566	-0.0486	-0.1261	-0.0562	-2.1625	-105.8	-203.9	-2.4329
Timoshenko's Theory	$\phi = 0$	0	-4.7460	0.0000	2.9456	-2.7139	2.7469	0.0000	2174.2	8965.3	0.0000
		0.25	-1.2307	0.0000	3.5196	-1.2115	2.8661	0.0000	2815.6	9536.8	0.0000
		0.50	3.0350	0.0000	4.2042	0.6924	2.9604	0.0000	3564.1	10069.0	0.0000
		0.75	8.6714	0.0000	5.0300	3.1742	3.0282	0.0000	4478.0	10577.0	0.0000
	$\phi = \pi/2$	0	0.2610	4.0601	-0.0656	-0.3017	-0.0559	-2.4608	-164.8	-222.8	-2.768
		0.25	0.3678	4.3612	-0.0646	-0.2685	-0.0554	-1.9987	-152.9	-217.1	-2.249
		0.50	0.3178	4.5464	-0.0589	-0.2625	-0.0551	-1.4416	-150.5	-215.4	-1.622
		0.75	0.5896	4.5793	-0.0485	-0.182[illegible]	-0.0548	-0.7995	-123.4	-205.6	-0.899

TABLE XIII

DYNAMIC RESPONSE FOR UNIT IMPULSE WITH IN-PLANE INERTIA

Comparison of Theories

Time = 0.0006 sec $P/P_c = 0.5$

Flugge's Theory

ϕ	$u \times 10^{12}$	$v \times 10^{5}$	$w \times 10^{2}$	$\epsilon_x \times 10^{5}$	$\epsilon_\phi \times 10^{4}$	$\gamma_{x\phi} \times 10^{12}$	σ_x	σ_ϕ	$\tau_{x\phi} \times 10^{5}$
0	4.3863	0.0000	4.2052	-0.2079	2.9856	0.0000	3288.70	10053.00	0.0000
$\pi/4$	-1.3503	-1.0792	0.2489	-0.5523	-0.0021	1.1629	-188.76	-69.21	1.3083
$\pi/2$	0.5073	4.4458	-0.0589	-0.1895	-0.0569	-0.2341	-128.00	-213.45	-0.2634
$3\pi/4$	0.3238	-1.5013	-0.0361	-0.1045	-0.0392	0.1412	-8.82	-120.53	-0.1589
	0.5995	0.0000	0.0180	0.2459	-0.0362	0.0000	42.27	-94.49	0.0000

Timoshenko's Theory

0	3.0350	0.0000	4.2042	0.6924	2.9604	0.0000	3564.1	10069.00	0.0000
$\pi/4$	-1.3883	-1.1953	0.2485	-0.4348	-0.0198	1.4390	-169.02	-115.69	1.6189
$\pi/2$	0.3178	4.5464	-0.0589	-0.2625	-0.0551	-0.1442	-150.53	-215.36	-0.1622
$3\pi/4$	0.2017	-1.5087	-0.0361	0.0513	-0.0400	0.0441	-27.73	-129.34	0.0496
π	0.549	0.0000	0.0180	0.2142	-0.0371	0.0000	30.52	-101.20	0.0000

TABLE XIV

EFFECT OF HYDROSTATIC PRESSURE AND LOADING AREA ON DYNAMIC RESPONSE FOR UNIT IMPULSE

Flugge's Theory with In-Plane Inertia Included

Time = 0.0006 sec ϕ = 0.0

$\epsilon_1 = \epsilon_2 = 2$

P/P_c	$u \times 10^{12}$	$v \times 10^5$	$w \times 10^2$	$\epsilon_x \times 10^5$	$\epsilon_\phi \times 10^4$	$\gamma_{x\phi} \times 10^{13}$	σ_x	σ_ϕ	$\tau_{x\phi} \times 10^6$
0	-2.7277	0.0000	2.9461	-3.3372	2.7508	0.0000	1968.3	8908.5	0.0000
0.40	2.8774	0.0000	3.9164	-0.9363	2.9459	0.0000	2998.1	9837.2	0.0000
0.60	6.3306	0.0000	4.5165	0.6686	3.0216	0.0000	3623.7	10273.0	0.0000
0.80	10.5790	0.0000	5.21620	2.6315	3.0823	0.0000	4355.7	10699.0	0.0000

$\epsilon_1 = \epsilon_2 = 4$

P/P_c	$u \times 10^{12}$	$v \times 10^5$	$w \times 10^2$	$\epsilon_x \times 10^5$	$\epsilon_\phi \times 10^4$	$\gamma_{x\phi} \times 10^{13}$	σ_x	σ_ϕ	$\tau_{x\phi} \times 10^6$
0	-5.0438	0.0000	10.3530	-8.1653	9.0096	0.0000	7380	29489	0.0000
0.40	11.8610	0.0000	13.9770	-1.3521	10.0576	0.0000	10858	33792	0.0000
0.60	22.596	0.0000	16.2100	3.4277	10.5435	0.0000	13018	35970	0.0000
0.80	35.860	0.0000	18.802	9.2771	11.0011	0.0000	15507	38172	0.0000

$P/P_c = 0.6$

ϵ_1, ϵ_2	$u \times 10^{12}$	$v \times 10^5$	$w \times 10^2$	$\epsilon_x \times 10^5$	$\epsilon_\phi \times 10^4$	$\gamma_{x\phi} \times 10^{13}$	σ_x	σ_ϕ	$\tau_{x\phi} \times 10$
2,2	6.3306	0.0000	4.5165	0.6686	3.0216	0.0000	3623.7	10273.0	0.0000
4,4	22.5960	0.0000	16.2100	3.4277	10.5435	0.0000	13018.0	35970.0	0.0000
8,8	69.471	0.0000	44.794	25.4101	27.2613	0.0000	39245	94865	0.0000
16,16	-92.041	0.0000	53.917	-43.092	46.237	0.0000	37437	151200	0.0000

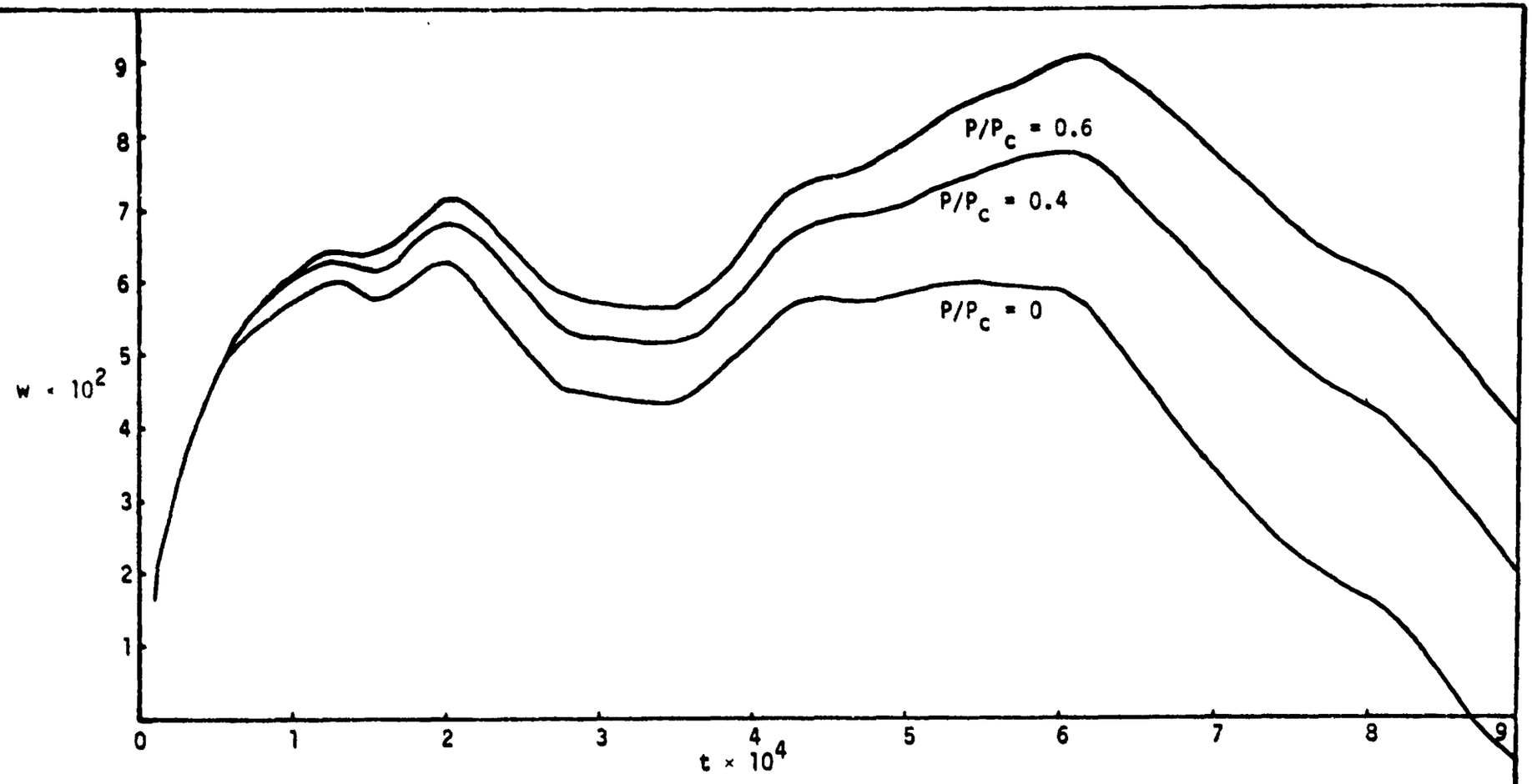

Figure 2. Radial Displacement versus Pressure for $\phi = 0$, $x = \ell/2$ at Various Values of Time

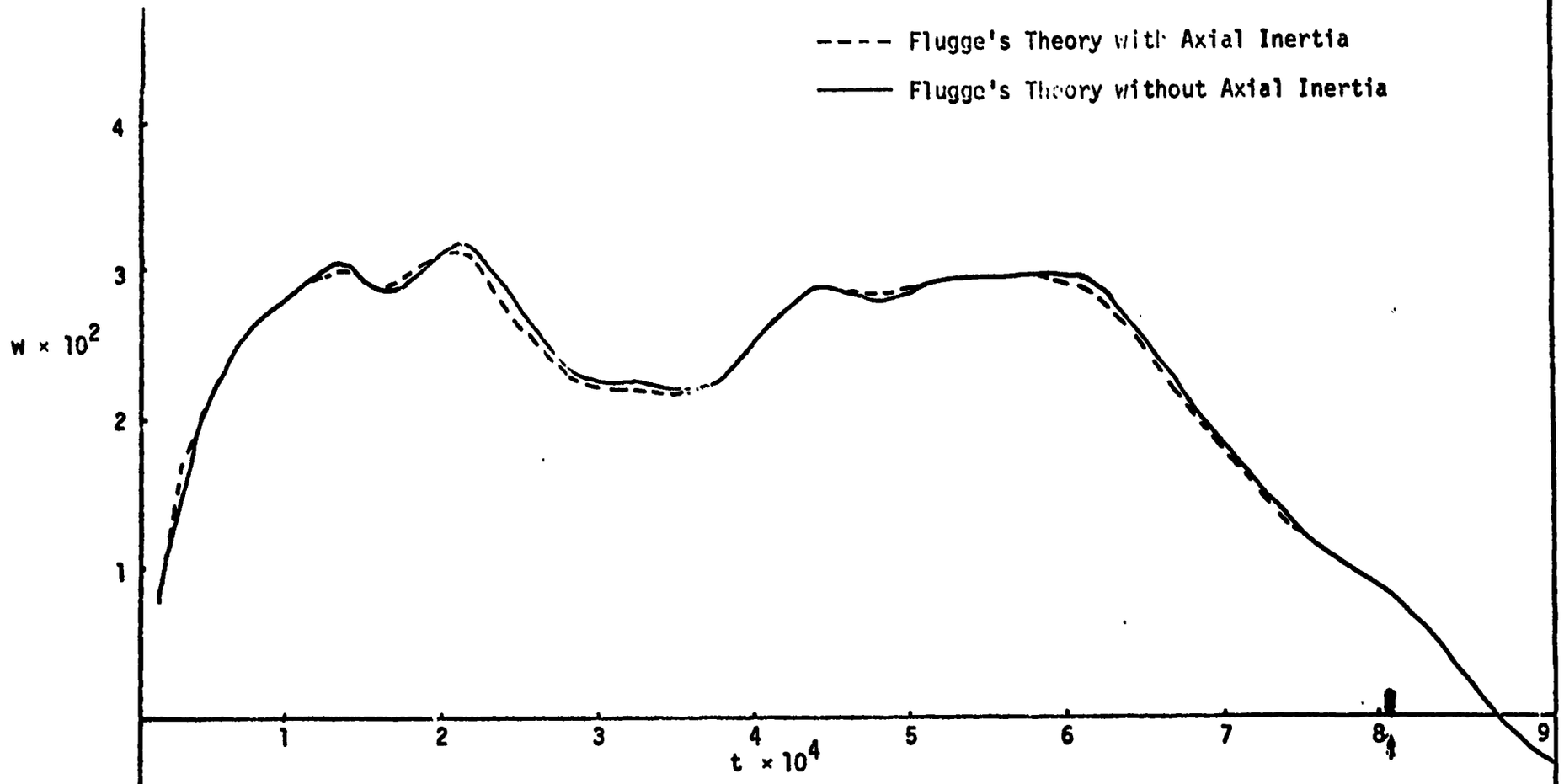

Figure 3. Radial Displacement versus Time for $P/P_c = 0$, $\phi = 0$, $x = \ell/2$ at Various Values of Time

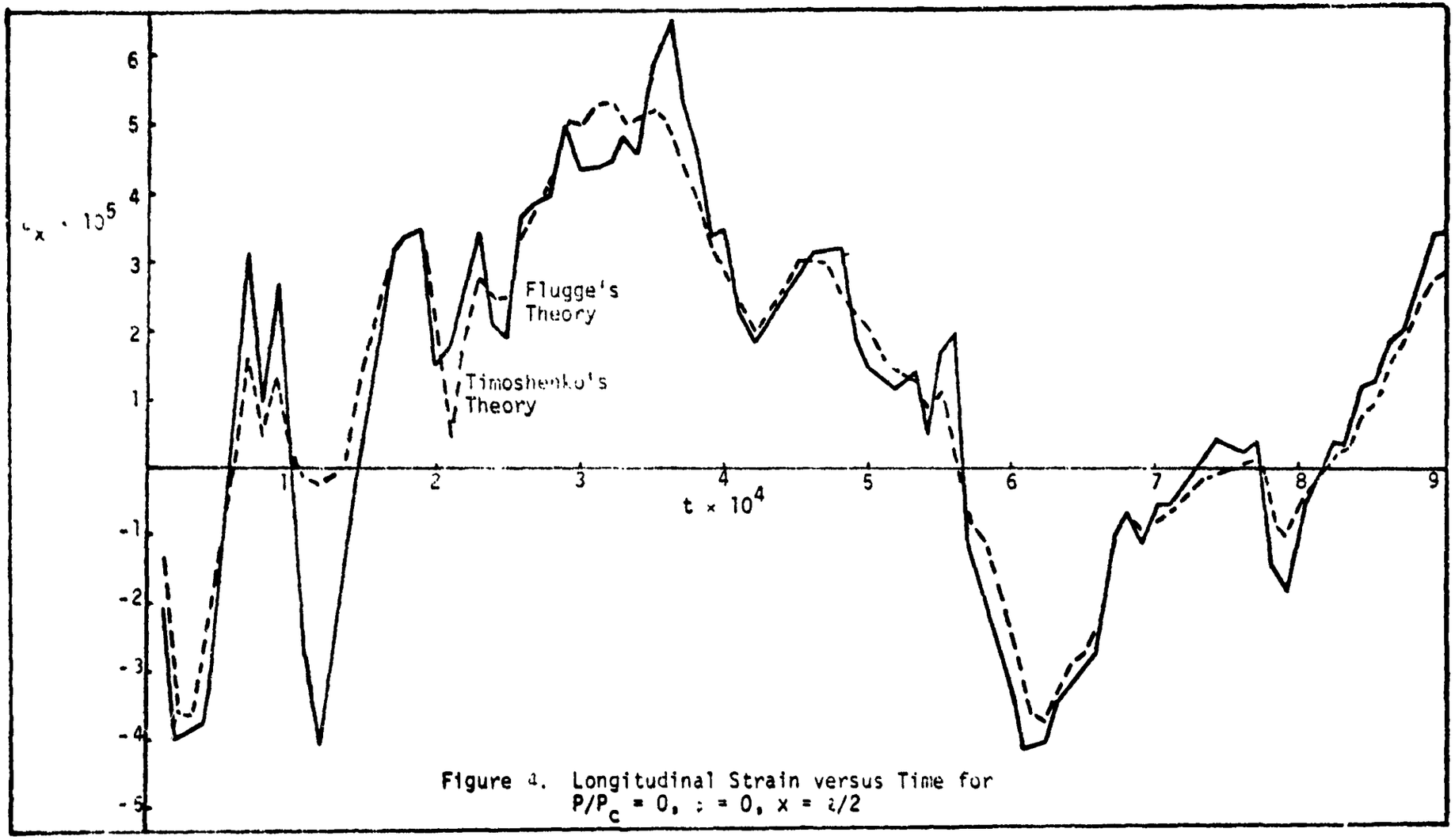

Figure 4. Longitudinal Strain versus Time for $P/P_c = 0$, $\zeta = 0$, $x = \ell/2$

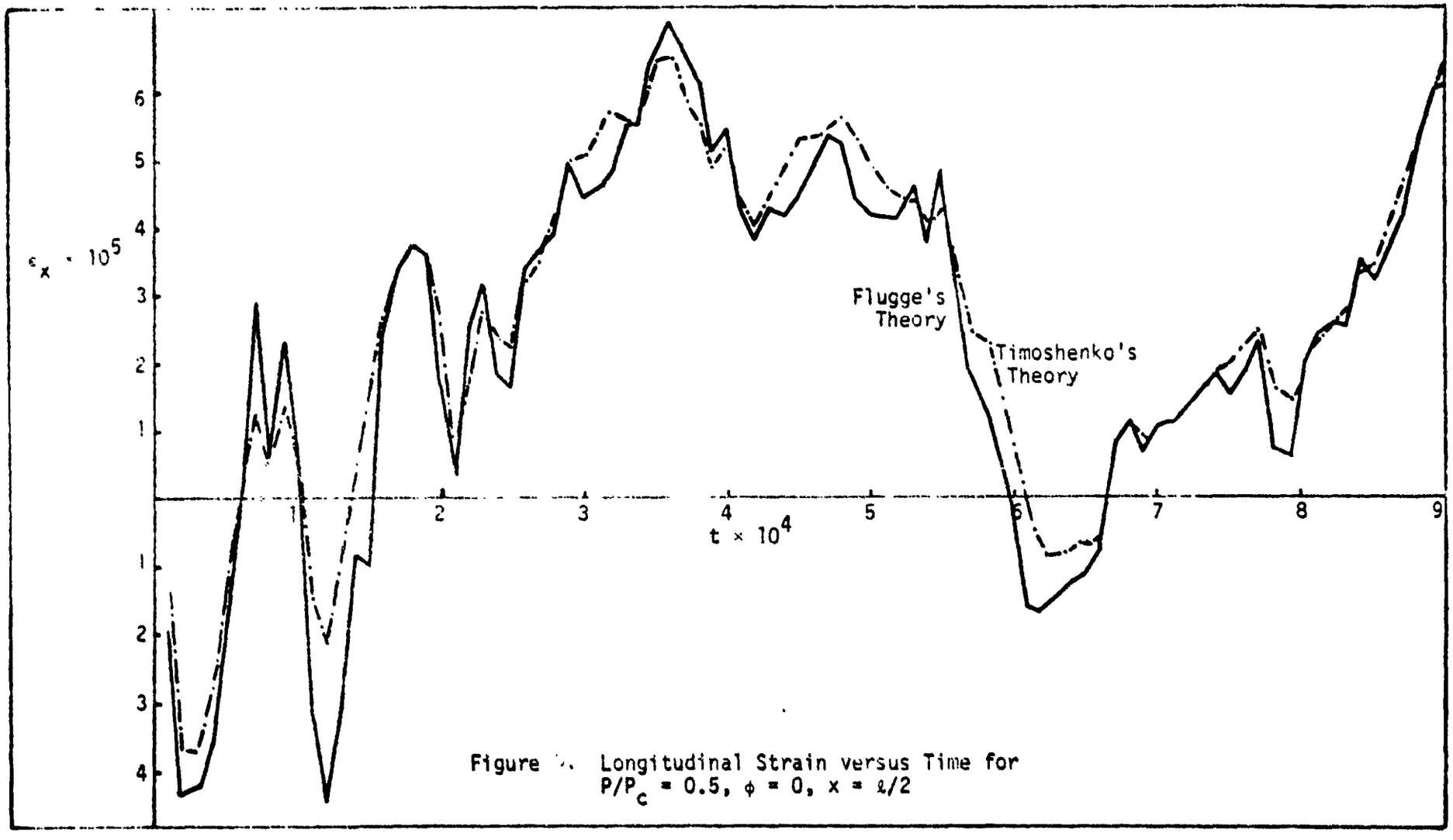

Figure 7. Longitudinal Strain versus Time for $P/P_c = 0.5$, $\phi = 0$, $x = \ell/2$

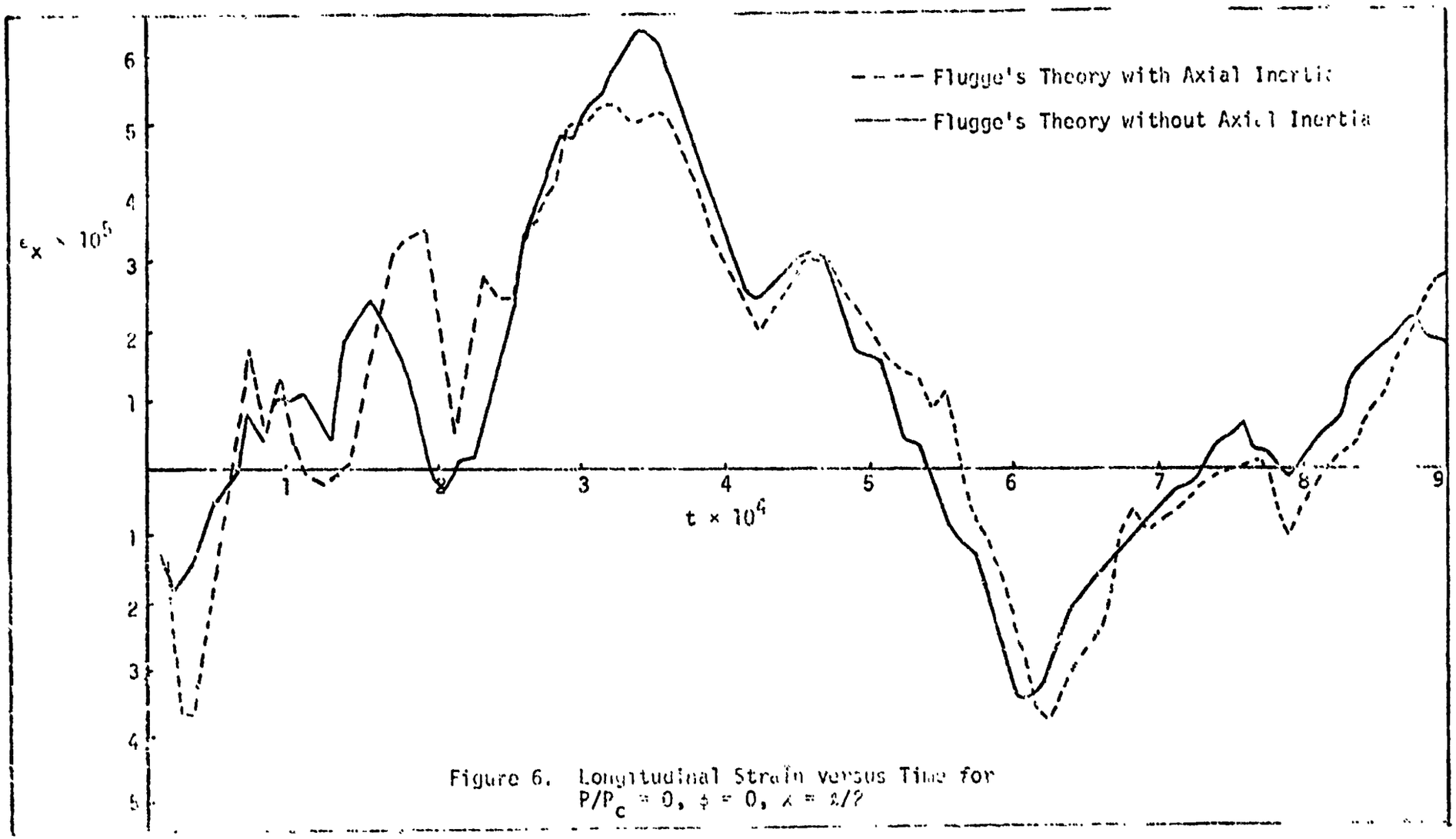

Figure 6. Longitudinal Strain versus Time for $P/P_c = 0$, $\phi = 0$, $x = \ell/2$

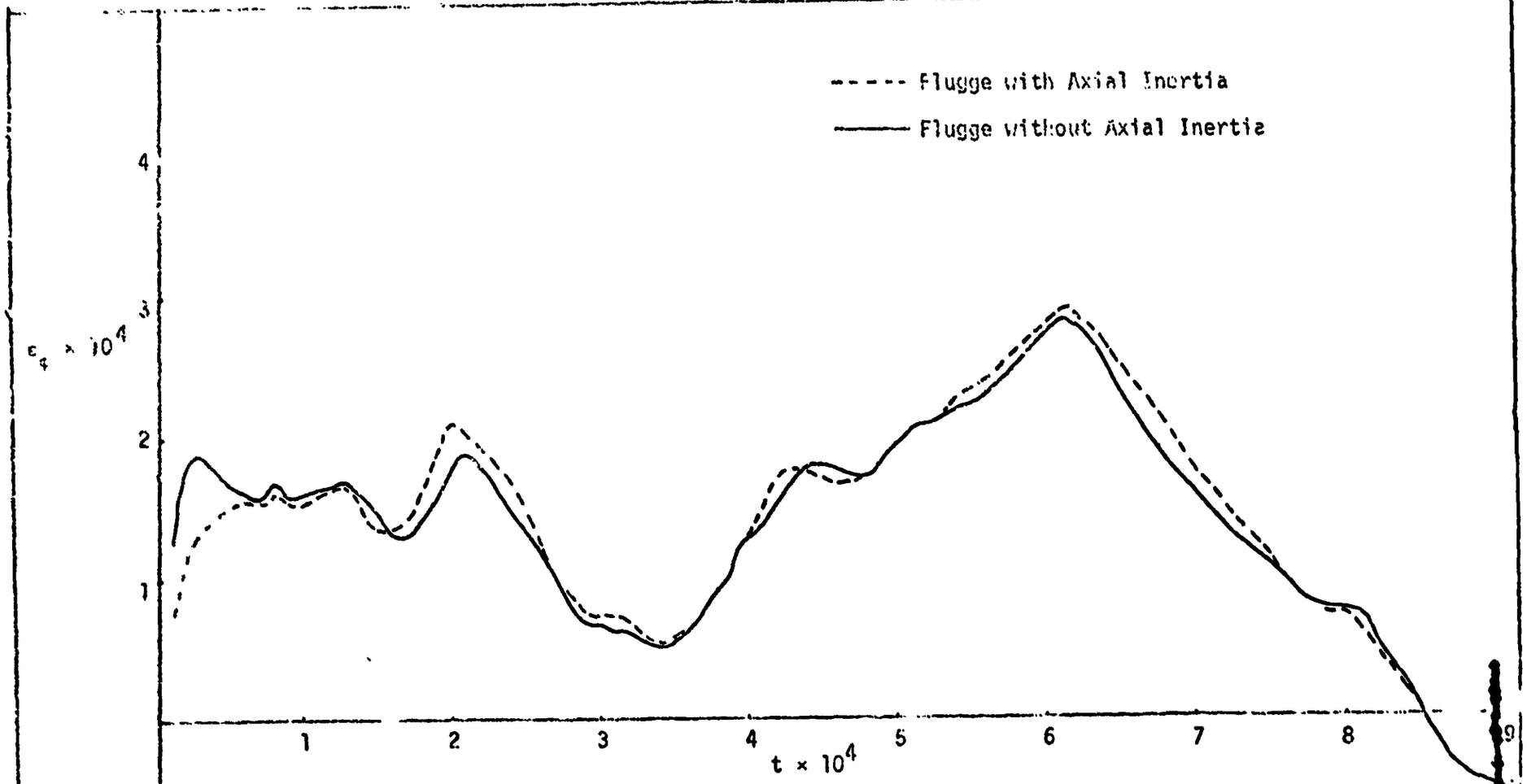

Figure 7. Circumferential Strain versus Time for $P/P_c = 0$, $\phi = 0$, $x = \ell/2$

Conclusions

Large hydrostatic pressures and small variations of impact area greatly affect the dynamic response of deep submersible hulls subjected to a localized impact loading.

For free vibrations deep hydrostatic pressures reduce the lower frequencies substantially while the higher frequencies are not appreciably affected. Hydrostatic pressures in the neighborhood of 50 percent of the buckling pressure can reduce the fundamental frequencies by 30 percent, while the higher frequencies, especially the second and third frequencies of the n, m mode will have no appreciable change.

Comparison of frequencies with the Flugge and Timoshenko theories show good agreement as illustrated in Tables I and II.

For forced vibrations as illustrated by a localized unit impulse, the following conclusions can be made:

a. Deep hydrostatic pressures have predominantly large effects on longitudinal displacements and strains. Consequently the longitudinal stresses, σ_x, will be more sensitive to change while the circumferential strains and stresses will increase moderately.

b. Shearing stresses experience moderate increases and are very small in magnitude.

c. Radial displacements and response times will have considerable increases as shown in Figure 3.

d. Small changes in the area of loading have tremendous influence on displacements and stresses as shown in Table XIV.

e. Comparison of theories indicates the following:

(1) The greatest discrepancy occurs in longitudinal displacements and strains.

(2) Within the area of impact, stresses, radial and circumferential displacements have good agreement, while those outside the area of impact can have large discrepancies.

(3) A good estimate of stresses, radial and circumferential displacements within the area of impact can be found by neglecting in-plane inertias.

References

[1] Flugge, W., Stresses in Shells, Springer-Verlag, Berlin, Germany, 1960.

[2] Timoshenko, S. P. and Gere, J. M., Theory of Elastic Stability, New York, McGraw-Hill Book Co., 1961, p. 496.

UNCLASSIFIED
Security Classification

DOCUMENT CONTROL DATA - R & D

Security classification of title, body of abstract and indexing annotation must be entered when the overall report is classified.

1. ORIGINATING ACTIVITY (Corporate author)
School of Engineering
University of Massachusetts
Amherst, Massachusetts 01002

2a. REPORT SECURITY CLASSIFICATION
UNCLASSIFIED

2b. GROUP

3. REPORT TITLE
IMPACT LOADING OF SUBMARINE HULLS

4. DESCRIPTIVE NOTES (Type of report and, inclusive dates)

5. AUTHOR(S) (First name, middle initial, last name)
Frederick J. Dzialo

6. REPORT DATE
February 1970

7a. TOTAL NO. OF PAGES
47

7b. NO. OF REFS
2

8a. CONTRACT OR GRANT NO
ONR-N00014-68-A-0146

b. PROJECT NO
In-house Project Number
N00014-68-A-0146-8

d.

9a. ORIGINATOR'S REPORT NUMBER(S)
THEMIS-UM-70-2

9b. OTHER REPORT NO(S) (Any other numbers that may be assigned this report)

10. DISTRIBUTION STATEMENT
Distribution of this document is unlimited.

11. SUPPLEMENTARY NOTES

12. SPONSORING MILITARY ACTIVITY
Department of Defense (Project THEMIS)

13. ABSTRACT

Following Flugge's exact derivation for the buckling of cylindrical shells, the equations of motion for dynamic loading of cylindrical shells subjected to hydrostatic and axial pressure have been formulated.

The equations of motion are applicable for long, short, or thick shells, and are very useful in calculating deflections and stresses when the impact loads are applied to comparatively small regions of the shell. The normal mode theory was utilized to provide dynamic solutions for the equations of motion.

Solutions are also provided for the Timoshenko-type theory, and comparisons are made between the two theories by considering and neglecting in-plane inertia forces.

Comparison of results is exemplified by a numerical example which considers the effect of hydrostatic pressure on the dynamic response of a shell simply supported by a thin diaphragm and subjected to a localized unit radial impulse.

DD FORM 1 NOV 65 1473 (PAGE 1)
S/N 0101-807-6811

UNCLASSIFIED
Security Classification